NASA/TM-2001-211264

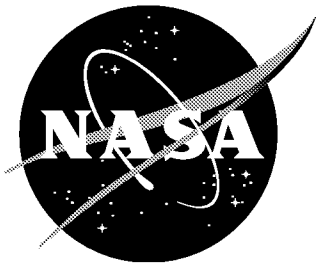

Effectiveness of Diffusion Barrier Coatings for Mo-Re Embedded in C/SiC and C/C

David E. Glass
Langley Research Center, Hampton, Virginia

Ravi N. Shenoy
Lockheed Martin Engineering & Sciences, Hampton, Virginia

Zengmei Wang
Chromealloy Gas Turbine Corporation, Orangeburg, New York

Michael C. Halbig
Glenn Research Center, Cleveland, Ohio

December 2001

The NASA STI Program Office ... in Profile

Since its founding, NASA has been dedicated to the advancement of aeronautics and space science. The NASA Scientific and Technical Information (STI) Program Office plays a key part in helping NASA maintain this important role.

The NASA STI Program Office is operated by Langley Research Center, the lead center for NASA's scientific and technical information. The NASA STI Program Office provides access to the NASA STI Database, the largest collection of aeronautical and space science STI in the world. The Program Office is also NASA's institutional mechanism for disseminating the results of its research and development activities. These results are published by NASA in the NASA STI Report Series, which includes the following report types:

- TECHNICAL PUBLICATION. Reports of completed research or a major significant phase of research that present the results of NASA programs and include extensive data or theoretical analysis. Includes compilations of significant scientific and technical data and information deemed to be of continuing reference value. NASA counterpart of peer-reviewed formal professional papers, but having less stringent limitations on manuscript length and extent of graphic presentations.

- TECHNICAL MEMORANDUM. Scientific and technical findings that are preliminary or of specialized interest, e.g., quick release reports, working papers, and bibliographies that contain minimal annotation. Does not contain extensive analysis.

- CONTRACTOR REPORT. Scientific and technical findings by NASA-sponsored contractors and grantees.

- CONFERENCE PUBLICATION. Collected papers from scientific and technical conferences, symposia, seminars, or other meetings sponsored or co-sponsored by NASA.

- SPECIAL PUBLICATION. Scientific, technical, or historical information from NASA programs, projects, and missions, often concerned with subjects having substantial public interest.

- TECHNICAL TRANSLATION. English-language translations of foreign scientific and technical material pertinent to NASA's mission.

Specialized services that complement the STI Program Office's diverse offerings include creating custom thesauri, building customized databases, organizing and publishing research results ... even providing videos.

For more information about the NASA STI Program Office, see the following:

- Access the NASA STI Program Home Page at ***http://www.sti.nasa.gov***

- E-mail your question via the Internet to help@sti.nasa.gov

- Fax your question to the NASA STI Help Desk at (301) 621-0134

- Phone the NASA STI Help Desk at (301) 621-0390

- Write to:
  NASA STI Help Desk
  NASA Center for AeroSpace Information
  7121 Standard Drive
  Hanover, MD 21076-1320

NASA/TM-2001-211264

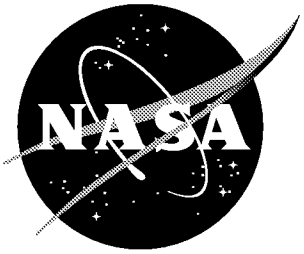

Effectiveness of Diffusion Barrier Coatings for Mo-Re Embedded in C/SiC and C/C

David E. Glass
Langley Research Center, Hampton, Virginia

Ravi N. Shenoy
Lockheed Martin Engineering & Sciences, Hampton, Virginia

Zengmei Wang
Chromealloy Gas Turbine Corporation, Orangeburg, New York

Michael C. Halbig
Glenn Research Center, Cleveland, Ohio

National Aeronautics and
Space Administration

Langley Research Center
Hampton, Virginia 23681-2199

December 2001

The use of trademarks or names of manufacturers in this report is for accurate reporting and does not constitute an official endorsement, either expressed or implied, of such products or manufacturers by the National Aeronautics and Space Administration, Lockheed Martin Engineering & Sciences, or Chromealloy Gas Turbine Corporation.

Available from the following:

NASA Center for AeroSpace Information (CASI)
800 Elkridge Landing Road
Linthicum Heights, MD 21090-2934
(301) 621-0390

National Technical Information Service (NTIS)
5285 Port Royal Road
Springfield, VA 22161-2171
(703) 487-4650

Effectiveness of Diffusion Barrier Coatings For Mo-Re Embedded in C/SiC and C/C

David E. Glass, NASA Langley Research Center, Hampton, VA 23681

Ravi N. Shenoy, Lockheed Martin Engineering & Sciences, Hampton, VA 23681

Zengmei Wang, Chromealloy Gas Turbine Corporation, Orangeburg, NY 10962-2515

and

Michael C. Halbig, NASA Glenn Research Center, Cleveland, OH 44135

Abstract

Advanced high-temperature cooling applications such as heat-pipe-cooled leading edges may often require the elevated-temperature capability of carbon/silicon carbide (C/SiC) or carbon/carbon (C/C) composites in combination with the hermetic capability of metallic tubes. In some applications, it may be advantageous to co-process metallic tubes with the composite. Under those conditions, it is important to understand the effect of the harsh environment of co-processing and additional thermal exposure on the metallic tubes in contact with carbon and silicon carbide. In this paper, the effects of C/SiC (using pyrolytic carbon (PyC) and CVI SiC processing steps) and C/C on tubes fabricated from several different refractory metals were evaluated. Though Mo, Nb, and Re were evaluated in the present study, the primary effort was directed toward two alloys of Mo-Re, namely, arc cast Mo-41Re and powder metallurgy Mo-47.5Re. Samples of these refractory metals were subjected to either the PyC/SiC deposition or embedding in C/C. $MoSi_2$(Ge), R512E, and TiB_2 coatings were included on several of the samples as potential diffusion barriers. Also, several of these samples were exposed to time at temperature in a vacuum as controls. The effects of the processing and thermal exposure on the samples were evaluated by conducting burst tests, microhardness surveys, and scanning electron microscopic examination (using either secondary electron or back scattered electron imaging and energy dispersive spectroscopy). The results showed that a layer of brittle Mo-carbide formed on the substrates of both the uncoated Mo-41Re and the uncoated Mo-47.5Re, subsequent to the C/C or the PyC/SiC processing. Both the R512E and the $MoSi_2$(Ge) coatings were effective in preventing not only the diffusion of C into the Mo-Re substrate, but also the formation of the Mo-carbides. However, Mo-silicide layers formed on the Mo-Re substrates as a result of the chemical interaction with both the R512E and the $MoSi_2$(Ge) coatings. This Mo-silicide layer grew with heat treatment time, albeit at a slower rate than the Mo-carbide layer in the uncoated condition, and thus reduced the effective thickness of the substrate. The development of lateral and transverse cracks in the R512E coating may have diminished the efficacy of that coating. For the Mo-47.5Re alloy, burst strength degraded moderately (relative to the uncoated condition) when the alloy tubes were coated with either $MoSi_2$(Ge) or TiB_2. The degradation in burst strength was more drastic subsequent to the coating followed by the PyC/SiC deposition, with the degradation from TiB_2 being more severe than from $MoSi_2$(Ge). $MoSi_2$(Ge) thus appeared to be more effective than TiB_2 as a diffusion barrier coating for Mo-47.5Re. However, none of the coatings were effective at preventing both C and Si diffusion without some degradation of the substrate.

Table of Contents

Introduction

Ceramic matrix or carbon/carbon composite (generically termed refractory composite herein) structures with embedded refractory-metal tubes may have numerous high-temperature applications. One such application is for light-weight heat-pipe-cooled leading edges with high-heat-flux capabilities, where refractory-metal tubes embedded in the refractory-composite structure serve as the containers for liquid-metal heat pipes. Refractory metals are utilized since they exhibit high melting points and high strengths at elevated temperatures, and can also withstand high processing temperatures required for manufacturing refractory-composite materials. In addition, they have the ability to be hermetically sealed enabling leak-free operation.

One of the complications encountered embedding a refractory-metal tube in a refractory-composite structure is lack of chemical compatibility between the two materials. Many of the refractory metals form carbides or silicides when in contact with carbon or silicon at elevated temperatures. The formation of carbides or silicides can lower the strength and ductility of the refractory metal. In addition, for heat-pipe applications, carbon or silicon may diffuse through the metal tube (i.e., heat-pipe container) and contaminate the heat pipe.

The Appendix presents a brief overview of literature that exists with respect to laboratory-based physical metallurgy aspects of refractory-metal compatibility with C and SiC, and the use of various diffusion barrier coatings to minimize the unfavorable interactions between the metals and the refractory composite. It is nevertheless important to study the effectiveness of diffusion barrier coatings on refractory metals and alloys of practical concern. Concurrently, it is also pertinent to evaluate the mechanical integrity of such systems comprising the refractory metal, the diffusion barrier coating, and the C or SiC environment before and after exposure to targeted high-temperature environments. It is with this objective that the present study was undertaken.

This report discusses an evaluation of the effects of pyrolytic carbon (PyC) followed by SiC deposition, and C/C on several different refractory metals. The PyC/SiC deposition, representing a C/SiC densification process, was applied by Honeywell Advanced Composites, Inc. (HACI), Newark, DE and the C/C processing was performed by Carbon-Carbon Advanced Technologies (C-CAT), Fort Worth, TX. The refractory alloys evaluated were Mo-Re, Mo, Nb, and Re which were formed into tubes by various processes. R512E (a proprietary Fe, Si, Cr-rich coating deposited by Hitemco), TiB_2, and $MoSi_2$(Ge) coatings were applied to the refractory metals as potential diffusion barriers. The methods of evaluating the effectiveness of the coatings and the effect of the C and SiC on the refractory metals were metallurgical characterization, including micorhardness and SEM, and burst test. The results of the metallurgical characterization are discussed first, followed by the results of the burst test.

Metallurgical Characterization

R512E, $MoSi_2$(Ge), and TiB_2 diffusion barrier coatings were metallurgically characterized on several different refractory metals for their ability to protect the metallic substrate from detrimental effects of C and Si diffusion and reactions. Samples were characterized in the uncoated, as-coated, and as-coated plus heat treated conditions, both with and without simulated C/C or C/SiC processing. A discussion of the characterization of each coating on various refractory-alloy tubes follows, with the results for the uncoated condition, wherever possible, serving as the baseline for comparison. The discussion details the changes in physical and chemical nature of the coatings and substrate microstructures in so far as these changes may ultimately affect the mechanical properties of the refractory-metal tubes. The metallurgical characterization was limited to the study of Mo, Mo-41Re, and Mo-47.5 Re tubes.

The appearance of the tubes after the PyC/SiC deposition was quite varied and appeared to be significantly affected by the presence of a diffusion barrier coating. A photograph of an uncoated AC Mo-41Re "D-shaped" tube (#17) after PyC/SiC deposition is shown in Fig. 1. The radius of the curved portion of the tube is 0.3 in, and the tube segment is 1-in. long. The surface of the tube was very rough, but in general, the PyC/SiC remained attached. This is in stark contrast to a TiB_2 coated AC Mo tube with PyC/SiC deposited, shown in Fig. 2, where the surface was very smooth, but the outer layer spalled. The "D-shaped" tube, again with a 0.3-in. radius, is shown in the center of Fig. 2, and pieces of PyC/SiC layers that spalled are shown above and below the tube.

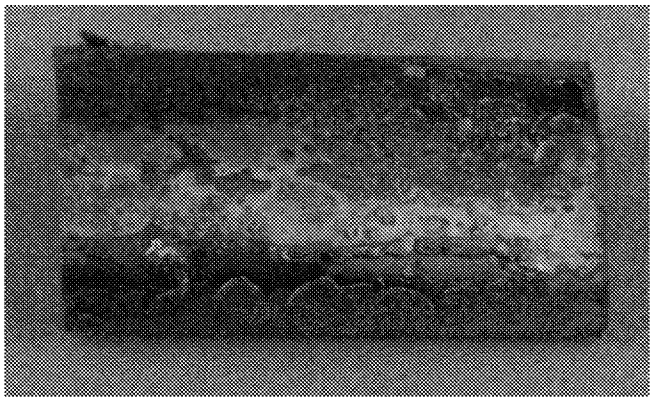

Fig. 1 Photograph of uncoated AC Mo-41Re "D-shaped" tube after PyC/SiC deposition (#17).

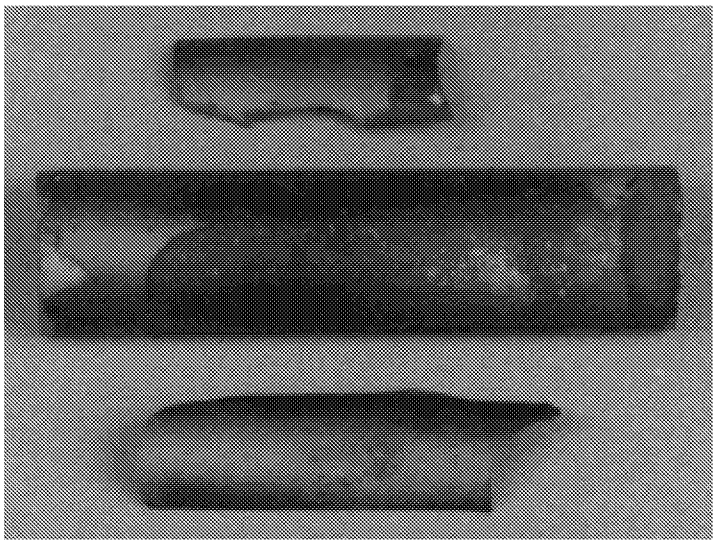

Fig. 2 Photograph of TiB_2 coated AC Mo "D-shaped" tube after PyC/SiC deposition (#24).

The uncoated PM Mo-47.5Re surface appearance after PyC/SiC deposition (Fig. 3) looked very different from the $MoSi_2$(Ge) coated PM Mo-47.5Re surface (Fig. 4) after PyC/SiC deposition. There were no large spalled sections in the uncoated condition (see Fig. 3), but a very rough surface. The surface roughness due to the PyC/SiC on the uncoated PM Mo-47.5Re tube (Fig. 3) was much larger than on the uncoated AC Mo-41Re tube (Fig. 1). As with the TiB_2 coated AC Mo tube with PyC/SiC deposition, the PyC/SiC on the $MoSi_2$(Ge) coated Mo-47.5Re tube spalled (see Fig. 4) and left a relatively smooth surface.

From the above photographs, it is clear that the PyC and SiC layers adhere to Mo and Mo-Re surfaces in significantly different manners depending on whether the tubes are coated or not with a diffusion barrier. Though the photographs indicate gross levels of adherence of the PyC and SiC

layers, they do not provide an indication of coating adequacy or inadequacy. On several coated samples, a spalled layer was present. The uncoated AC Mo-41Re, though it had a very rough surface, did not have significant spallation or flakes. Finally, it should be noted that the spalling of the PyC/SiC would be very different if the tubes were embedded and processed in a fiber preform.

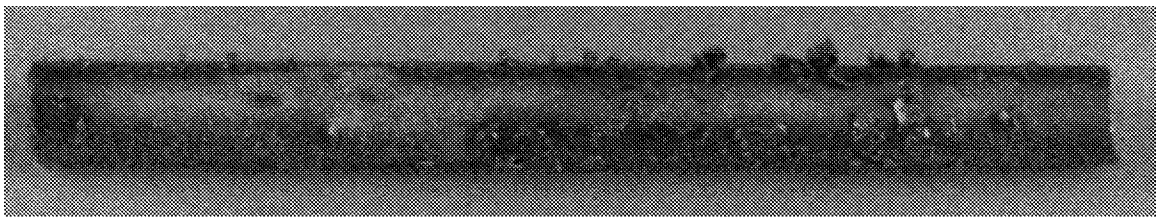

Fig. 3 Photograph of uncoated PM Mo-47.5Re tube after PyC/SiC deposition (#28). (Outer tube diameter is 0.197 in.)

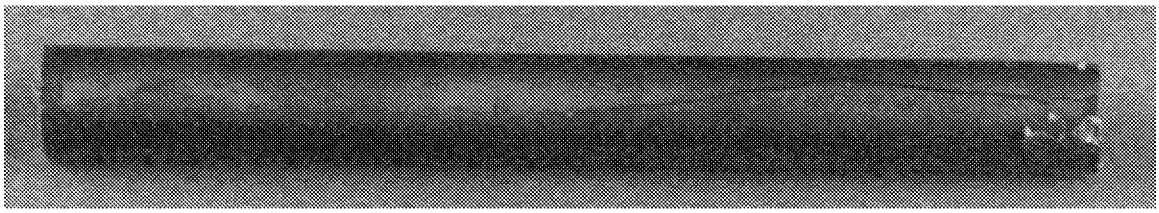

Fig. 4 Photograph of $MoSi_2$(Ge) coated PM Mo-47.5Re tube after PyC/SiC deposition (#23). (Outer tube diameter is 0.197 in.)

Materials and Coatings

The variables in this study were the refractory metals and alloys that were formed into thin wall tube specimens, protective coatings, environment (constituent materials from C/C or PyC/SiC processing), and the thermal exposure time and temperature. Each of these variables significantly influenced the metallurgical condition and mechanical properties of the material.

A full factorial test matrix, attempting to study the interplay of all the various materials, processes, and heat treatment variables, was not feasible for this study so only selected combinations of the variables were evaluated. The scope of this investigation in relation to metals and alloys, protective coatings, environment (C and/or SiC), and heat treatment time and temperature used in the study, in given in Table 1. Table 1 indicates the conditioning of the tube (as received, coated with PyC/SiC, embedded in C/C, and exposure for some time at a specific temperature, T(t)).

The refractory metals and alloys used in the metallurgical characterization study included arc cast (AC)- and powder metallurgy (PM)- derived products. Both "D-shaped" and circular tubes were evaluated. The different refractory metals evaluated were:

- AC Mo-41Re
- PM Mo-47.5Re
- AC Mo

The AC Mo and Mo-Re tubing was drawn by Thermo Electron Tecomet in Wilmington, MA and the PM Mo-47.5Re tubes were fabricated by Rhenium Alloys, Elyria, OH.

The following three diffusion barrier coatings were evaluated:

- TiB_2
- $MoSi_2$(Ge)
- R512E

The TiB_2 coating was applied by Applied Technologies Coatings, Fort Worth, TX, using the CVD process. The $MoSi_2$(Ge) coating was applied by Dr. Robert Rapp at Ohio State University, using the pack cementation process. $MoSi_2$(Ge) is essentially a $MoSi_2$ coating doped with Ge to improve the coefficient of thermal expansion (CTE) compatibility when applied to certain refractory metals. The R512E coating is an Fe, Si, Cr-rich coating, previously utilized on Mo-41Re embedded in C/C[1], and was applied by Hitemco, Bethpage, NY using a slurry process.

The various refractory metal tubes were evaluated in the following conditions:

- uncoated (no diffusion barrier coating)
- coated (TiB_2, $MoSi_2$(Ge), or R512E)
- PyC/SiC deposition
- embedded in C/C
- exposed for 200 hours at 2000°F in a vacuum after PyC/SiC deposition (both coated with a diffusion barrier coating and uncoated)
- exposed for 0.5, 2.5, 8, and 32 hours at 2300°F in a vacuum after R512E coating and embedding in C/C.

Table 1. Material and Processing Conditions Characterized

	Refractory Metal Tube		
	AC Mo-41Re	PM Mo-47Re	AC Mo
Uncoated			
	as received		
	as received + T(t)	as received	as received
	PyC/SiC	PyC/SiC	PyC/SiC
	PyC/SiC + T(t)	PyC/SiC + T(t)	
	C/C + T(t)		
Coated			
$MoSi_2$(Ge)	as received	as received	as received
	PyC/SiC		PyC/SiC
	PyC/SiC + T(t)	PyC/SiC + T(t)	PyC/SiC + T(t)
R512E	as received		
	C/C		
	C/C + T(t)		
	PyC/SiC		
TiB_2		as received	as received
		PyC/SiC	PyC/SiC
		PyC/SiC + T(t)	PyC/SiC + T(t)

R512E Coating

The Hitemco R512E coating on AC Mo-41Re was characterized in several different conditions by scanning electron microscopy (SEM) and microhardness. The Mo-41Re was characterized in the following conditions, with the specimen number in parenthesis following the conditioning:

- Uncoated (#5)
- Uncoated, embedded in C/C, and exposed at 2300°F for 8 hr (#57)
- As coated with R512E (#50)
- Coated with R512E and embedded in C/C (#51)
- Coated with R512E, embedded in C/C, and exposed at 2300°F for 0.5 hr (#52)
- Coated with R512E, embedded in C/C, and exposed at 2300°F for 2.5 hr (#53)

- Coated with R512E, embedded in C/C, and exposed at 2300°F for 8 hr (#54)
- Coated with R512E, embedded in C/C, and exposed at 2300°F for 32 hr (#55)

Back scatter electron (BSE) images were obtained together with x-ray elemental maps to identify morphology and chemistries of the coating and substrate. The BSE images rely on the atomic number contrast in order to reveal details in a microstructure. Microhardness depth profiles, using a 25 g load in conjunction with a Knoop indenter, were performed to corroborate the chemistry information and to estimate the depth of contamination in the substrate. The contamination in the substrate was due to elemental diffusion consequent to the coating process and/or the 2300°F heat treatment.

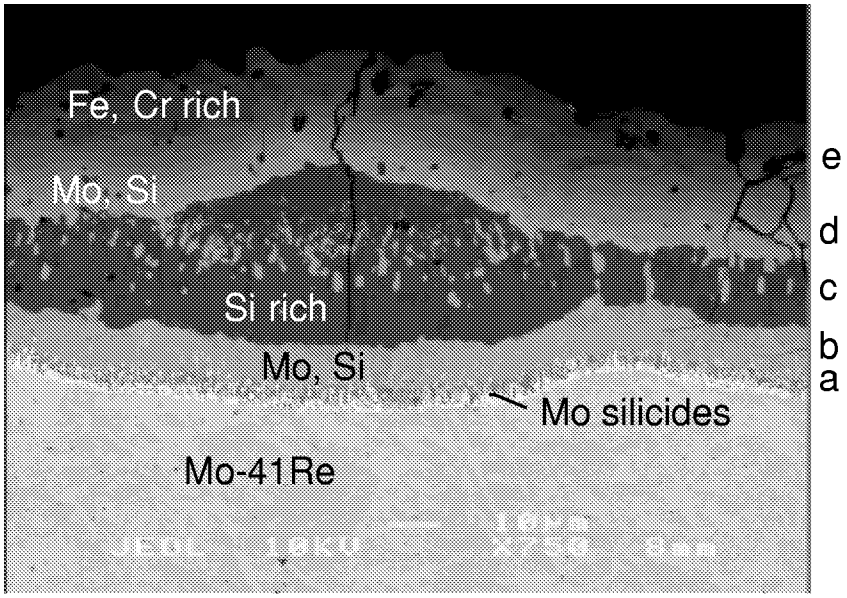

Fig. 5 SEM micrograph of R512E-coated AC Mo-41Re in the as-coated condition (#50).

The R512E coating was composed of at least five layers, as shown in Fig. 5. The layered structure resulted from the coating process step that involved heating the coated substrate at approximately 2600°F for 2 hr. X-ray elemental maps of the coating are shown in Fig. 6, where the light colored dots represent a high concentration of the specified element. Layer 'a' in Fig. 5 (~4-μm thick), immediately in contact with the Mo-Re substrate, was substantially rich in Mo and Si, and appeared to be composed of a mixture of Mo_3Si and Mo_5Si_3. Layer 'b' (~10-μm thick), adjacent to layer 'a', was generally rich in Mo and Si, and had a hardness of 1307±94 KHN. Layer 'c' (~25-μm thick) was substantially enriched in Si, and had a high hardness of 2261±336 KHN. Layer 'd' appeared to be similar in chemistry to layer 'b'. Layer 'e', with a hardness of 1424±147 KHN, was predominantly Fe and Cr. The elemental x-ray maps for this layer indicated that compositional gradients existed with respect to both Fe and Cr. The scatter in the hardness values for these various layers stems from chemical inhomogeneities, and thus attested to the complex nature of the layered structure of the coating.

In contrast to the inherently complex R512E coating layer, the Mo-Re substrate was predominantly a single phase microstructure with a grain size of ~40 μm and a hardness of 415±26 KHN. The hardness scatter in the substrate is indicative of hardness differences due to grain-to-grain differences in orientation of Mo-Re crystals. The presence of inter-dendritic shrinkage cavities in the general microstructure appeared to be intrinsic to the process of arc casting the alloy billets prior to their fabrication into Mo-Re tubes. It is pertinent to note that the sharp edges of these inter-dendritic cavities are potential stress risers, and hence their presence is detrimental to a

ductility-based mechanical property such as burst strength. In other words, in the absence of these shrinkage cavities, the strength of uncoated Mo-Re is likely to be significantly higher.

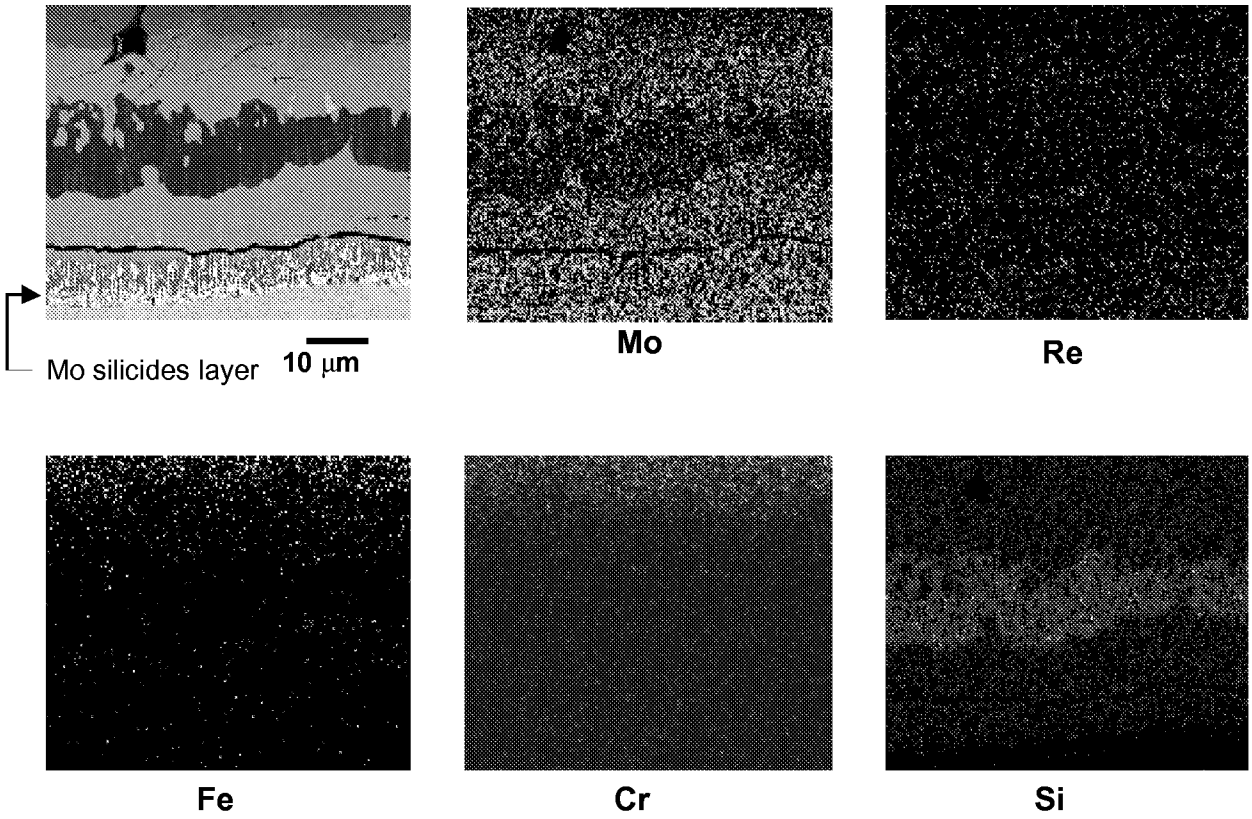

Fig. 6 Elemental x-ray maps of R512E-coated AC Mo-41Re (#50).

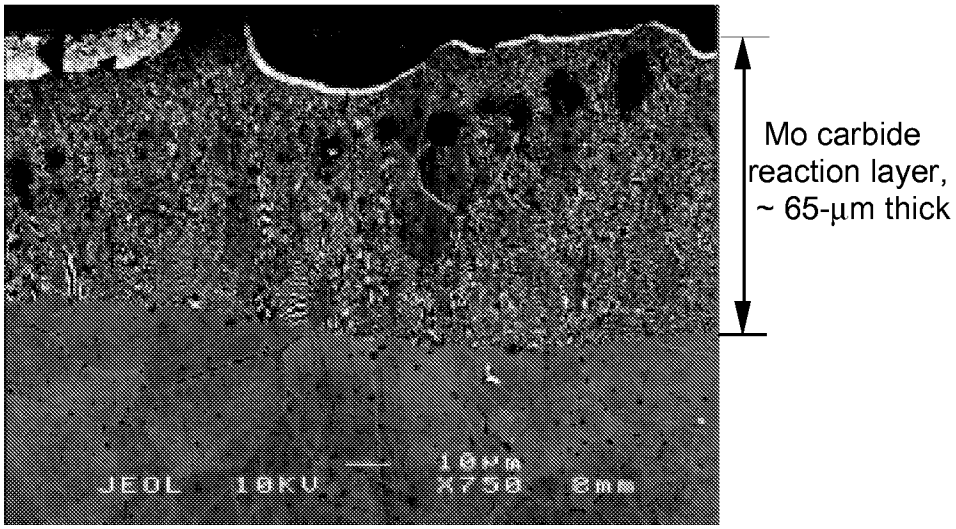

Fig. 7 SEM micrograph of uncoated AC Mo-41Re with C/C deposition (#57). Inter-dendritic shrinkage cavities can be seen in the Mo-Re substrate.

The BSE images of the uncoated Mo-41Re tube embedded in C/C revealed the presence of a ~65-μm thick Mo-carbide region in the substrate adjacent to the C/C interface (see Fig. 7). This transformed region, with a lamellar morphology, had a hardness value in the range of 1760 to 2430

KHN. In order to rationalize the development of this hard region in the uncoated sample, it is instructive to view the binary Mo-C phase diagram (see Fig. 8) for plausible interactions of C with Mo in the substrate. The isotherm corresponding to the 2300°F heat treatment temperature typical of the C/C deposition process is superimposed on the figure. The phase diagram indicates the presence of a eutectoid reaction at 2192±36°F for compositions beyond 5.7 wt.% C. The decomposition products on cooling through a eutectoid transformation temperature are typically associated with a characteristic lamellar morphology. The eutectoid constituent in the Mo-C system is comprised of a mixture of αMo_2C and MoC. The carbides are hard and brittle. In the absence of a coating, therefore, substantial C enrichment of the substrate can take place rapidly during the 2300°F heat treatment, thus rendering a significant portion of the normally ductile cross-section brittle through carbide formation. The presence of such a brittle layer can rapidly degrade the burst strength. Beyond the carbidic region, the hardness profile in the substrate rapidly leveled off to the Mo-41Re base hardness of 412±30 KHN (which incidentally, was the same as for the R512E coated condition discussed previously).

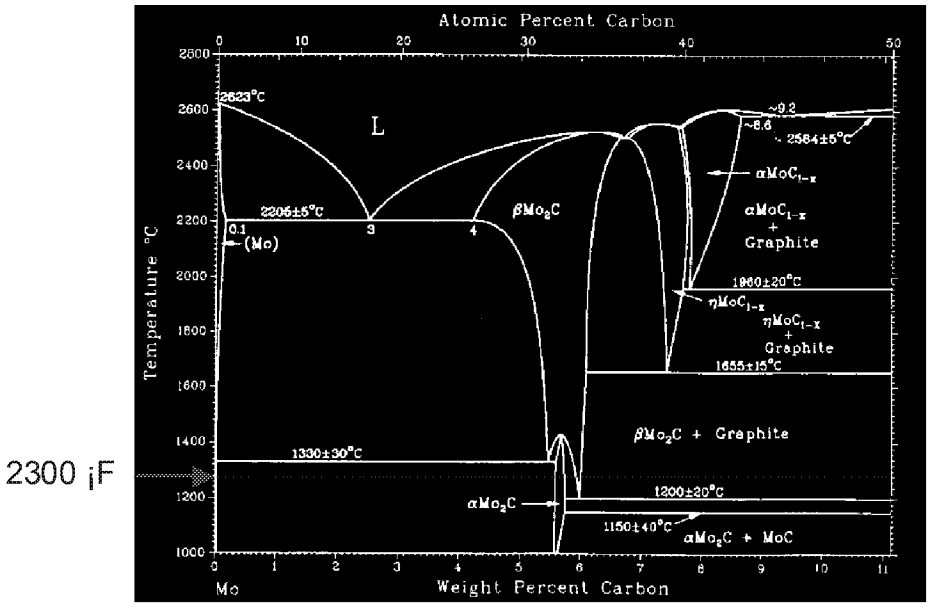

Fig. 8 Mo-C binary phase diagram.

Hardness depth profiles of the Mo-41Re substrate for several different conditions are shown in Fig. 9. Note that the origin of the hardness profile is at the substrate/C/C interface (for the uncoated sample) or at the substrate/R512E interface (for the coated samples). The uncoated sample showed a carbide region over the first ~65 μm depth (see Fig. 7). The thickness of the Mo-carbide region, as determined from the BSE image, was fully corroborated by the plateau region of the depth profile in Fig. 9. This plateau region had high hardness relative to the substrate, and can therefore be expected to be less ductile than the Mo-Re substrate. All of the coated samples, on the other hand, indicated no significant increase in hardness of the substrate (with measurements starting below the Mo-silicide layer). It is thus apparent that the R512E coating did significantly prevent C from diffusing into the Mo-Re substrate, but at the cost of a high hardness Mo-silicide layer formation.

The hardness of the substrate varied slightly with coating and exposure time as shown in Fig. 10. The Mo-41Re in the uncoated condition, with a substrate hardness of 474±36 KHN, had a microstructure similar to that of the Mo-Re substrate in the R512E-coated sample. The inherently lower hardness of the coated sample compared to that for the uncoated condition suggests that the coating process (together with the firing at 2600°F) brings about a thermally induced softening of

the Mo-Re substrate as shown in Fig. 10. The moderate but measurable increase in the substrate hardness for the coated and exposed samples (with respect to that for the as-coated condition) suggests small levels of possible Si contamination.

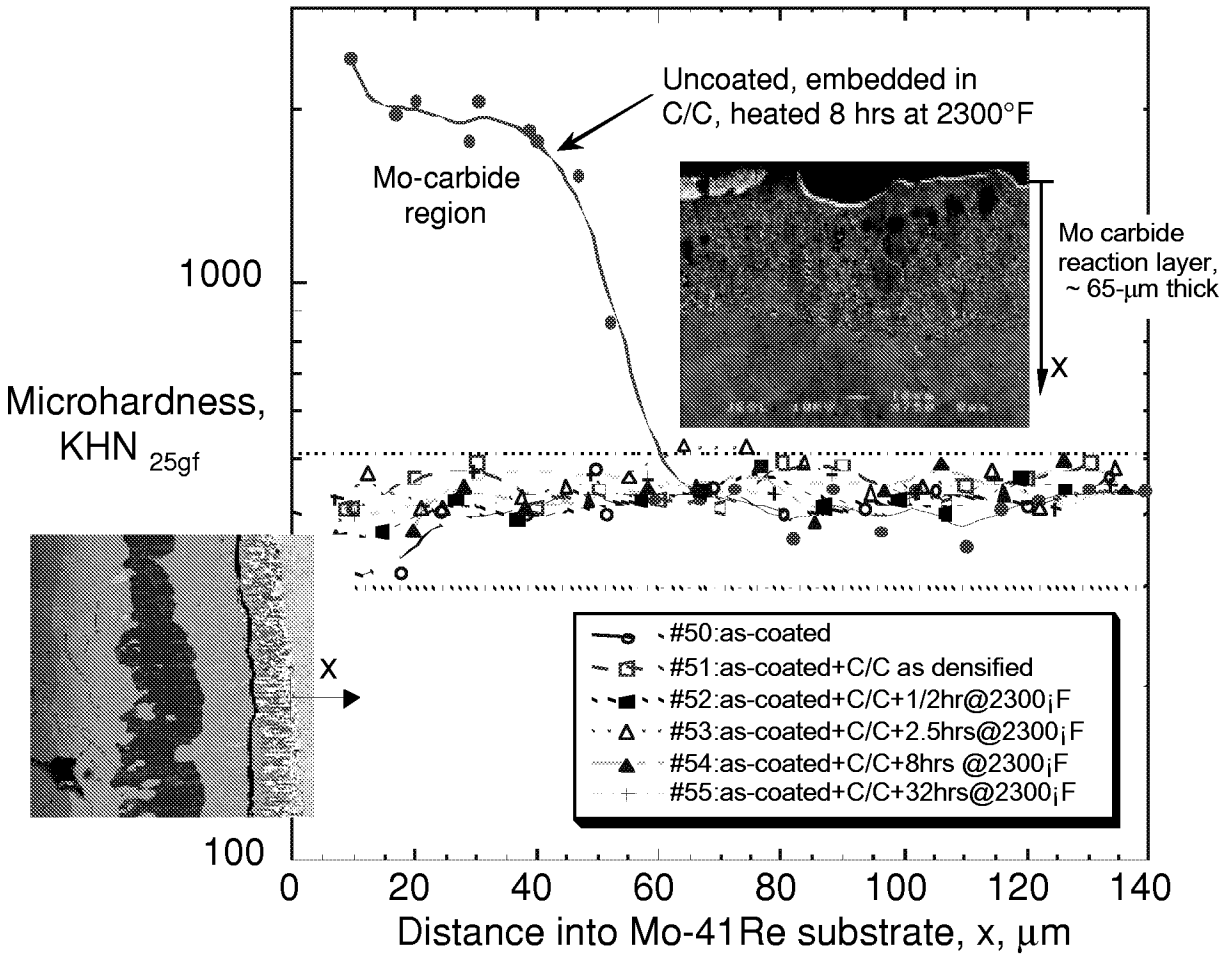

Fig. 9 Microhardness depth profile of coated and uncoated Mo-41Re substrate.

Increasing the time of the heat treatment affected both the coating characteristics and the Mo-Re substrate. The samples coated with R512E, unlike the uncoated sample embedded in C/C, showed no carbidic region. The presence of the R512E coating thus appeared to prevent C from diffusing into the Mo-Re substrate. For all the heat treatment times, the R512E coating on the 2300°F exposed samples embedded in C/C showed qualitatively the same layered structure as for the as coated condition discussed above. However, the thickness of the Mo-silicide layer (corresponding to Mo_3Si and Mo_5Si_3) increased with increasing exposure time, as shown in Fig. 11. Correspondingly, there was a decrease in the Si-enriched layer. This clearly suggests that with increasing duration of the 2300°F exposure, diffusion gradients were set up such as to cause depletion of Si from the Si-rich layer and a concomitant growth of the Mo-silicide layer on the substrate. The growth of this brittle silicide layer was at the expense of the Mo-Re substrate.

In contrast to a thickness of ~65 μm of the carbide layer that developed in the uncoated sample during 8 hr of heat treatment at 2300°F, only ~5.5 μm of the Mo-silicide layer developed during the same duration for the coated sample. The hardness depth profiles in the substrate indicated no significant concentration gradients due to Si diffusion. However, the moderate but

measurable increase in the substrate hardness with respect to that for the as-coated condition suggests (see Fig. 10) small levels of possible Si contamination.

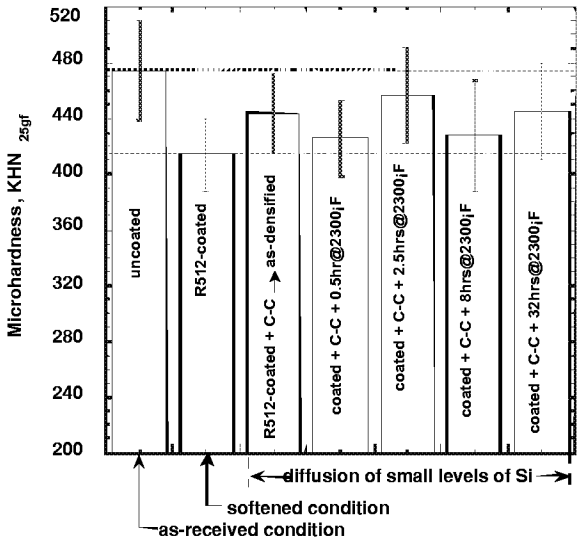

Fig. 10 Microhardness of AC Mo-41Re substrate.

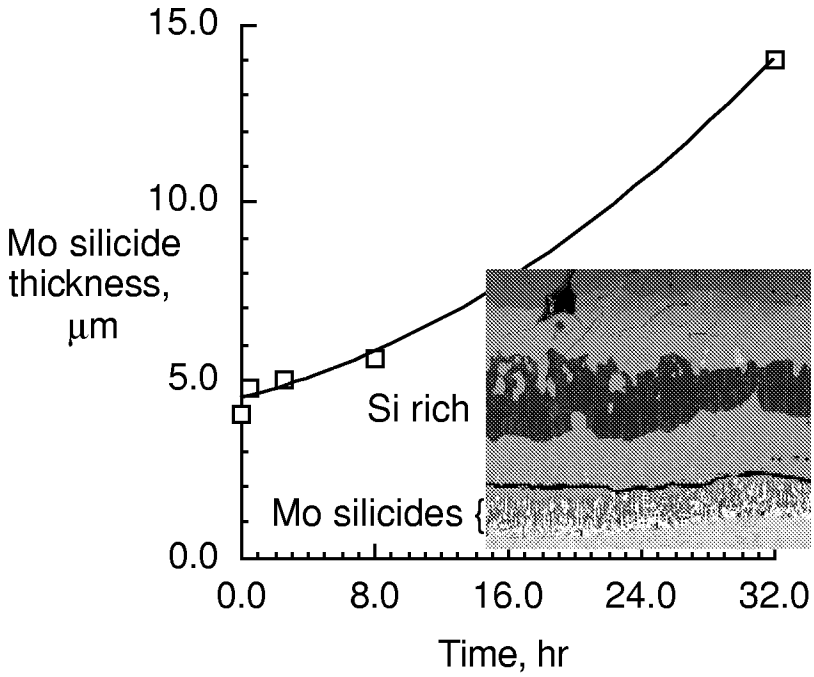

Fig. 11 Mo-silicide layer thickness in AC R512E-coated Mo-41Re as a function of time at 2300°F.

An SEM micrograph of an R512E-coated Mo-41Re sample embedded in C/C and heated for 0.5 hr at 2300°F in a vacuum is shown in Fig. 12. It is readily seen that both lateral and transverse cracks developed in both the R512E coating and the Mo-silicide layer. These cracks tended to grow with increasing time of heat treatment. Thus, eventually the coating became ineffective in

preventing C diffusion into the substrate. In addition, the silicide layer also tended to debond, thus increasing the thermal resistance to heat flow.

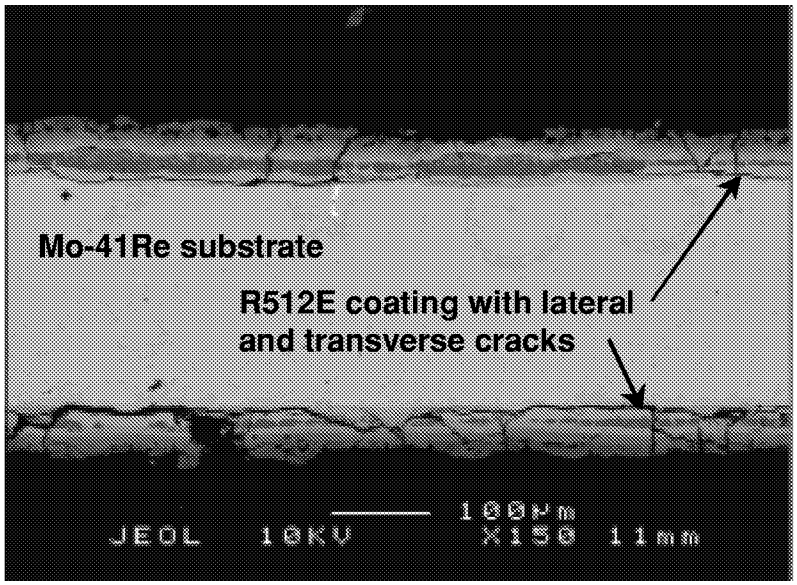

Fig. 12 SEM micrograph of R512E-coated AC Mo-41Re embedded in C/C and heated for 0.5 hr at 2300°F (#52).

$MoSi_2$(Ge) Coating

A Ge-doped $MoSi_2$ coating was applied to AC Mo-41Re, AC Mo, and PM Mo-49.5Re by Dr. Robert Rapp of Ohio State University. The $MoSi_2$(Ge) coating was applied by a pack cemetation process. After the coating was applied, PyC/SiC was deposited on some of the tubes by HACI. An analysis of the Mo and Mo-Re alloys, with and without the coating, follows.

AC Mo-41Re

AC Mo-41 Re tubes with and without the $MoSi_2$(Ge) coating were characterized in the following conditions:

- Uncoated (#5)
- Uncoated with PyC/SiC deposition (#17)
- Uncoated with PyC/SiC deposition and exposed at 2000°F for 200 hr (#31)
- $MoSi_2$(Ge)-coated (#13)
- $MoSi_2$(Ge)-coated with PyC/SiC deposition (#15)
- $MoSi_2$(Ge)-coated with PyC/SiC deposition and exposed at 2000°F for 200 hr (#16)

On the uncoated sample with PyC/SiC deposition, a Mo-carbide reaction layer formed adjacent to the Mo-Re substrate. It is thus clear that in the absence of a protective barrier coating, the PyC/SiC processing was associated with undesirable substrate/PyC/SiC reaction products. The Mo-carbide layer was brittle and thus represented a loss of effective load-bearing cross section for the substrate. Further, the thickness of the Mo-carbide layer increased from an initial 5 μm to 20 μm after the 2000°F/200 hr heat treatment (see Fig. 13). In contrast, on the coated sample (see Fig. 14) the $MoSi_2$(Ge) coating appeared to be effective in preventing carbon from the PyC/SiC layer from diffusing into, and reacting with, the Mo-Re substrate. As a result, no Mo-carbide layer was observed. On the other hand, Si from the $MoSi_2$(Ge) coating appeared to react with Mo in the Mo-Re substrate forming a Mo-silicide layer. Further, the thickness of this reaction layer increased

with heat treatment time. As a result of the Mo-silicide layer, and perhaps because of its CTE incompatibility with the substrate, extensive cracks developed at the coating/substrate interface in the 2000°F/200 hr heat treated sample.

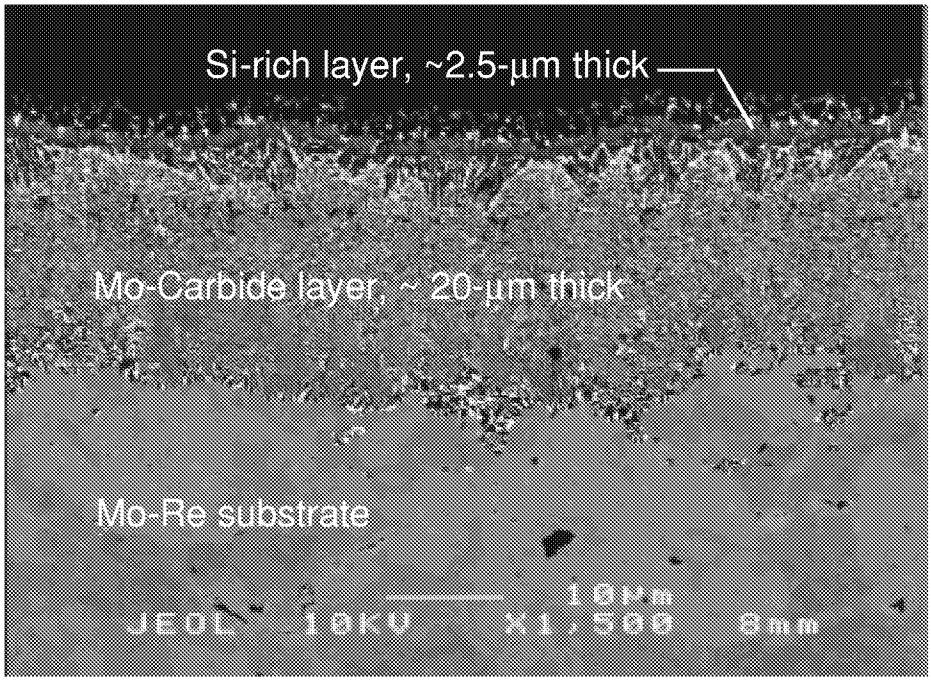

Fig. 13 SEM micrograph of uncoated AC Mo-41Re with PyC/SiC deposition and heated at 2000°F for 200 hr (#31).

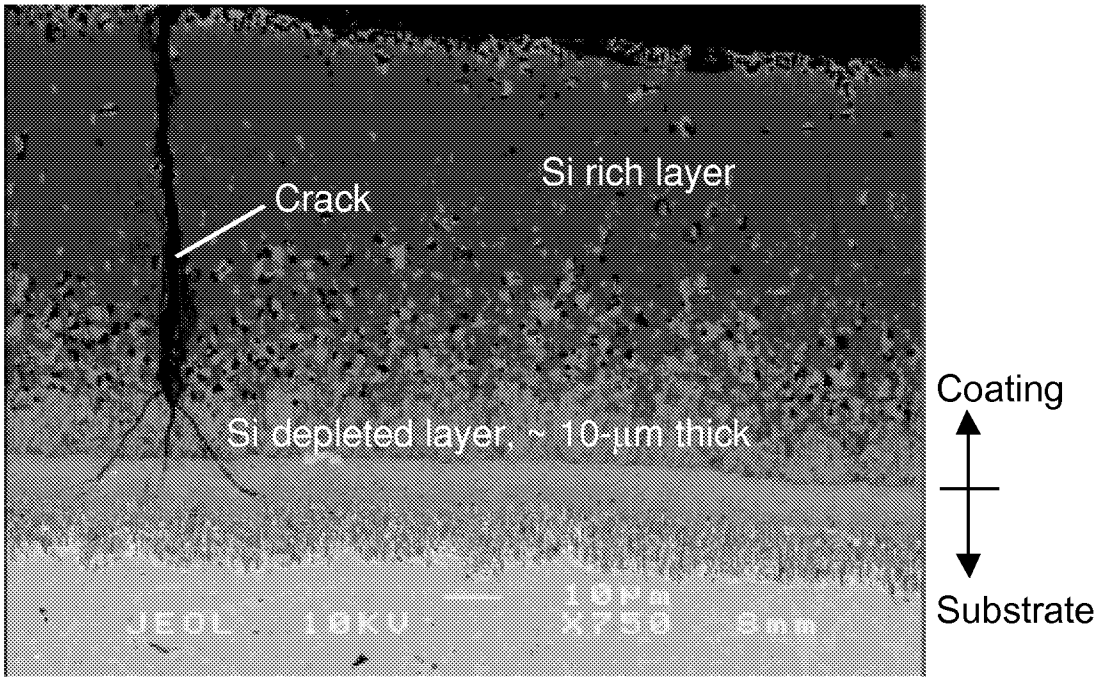

Fig. 14 SEM micrograph of $MoSi_2$(Ge)-coated AC Mo-41Re with PyC/SiC deposition and heated at 2000°F for 200 hr (#16).

PM Mo-47.5Re

PM Mo-47.5Re samples with and without $MoSi_2$(Ge) coatings were characterized in the following conditions.

- Uncoated (#3)
- Uncoated with PyC/SiC deposition (#28)
- Uncoated with PyC/SiC deposition and heat treated in a vacuum at 2000°F for 200 hours (#29)
- Coated with 17 μm $MoSi_2$(Ge) (#2)
- Coated with 17 μm $MoSi_2$(Ge) with PyC/SiC deposition (#23)
- Coated with 17 μm $MoSi_2$(Ge) with PyC/SiC deposition and heat treated in a vacuum at 2000°F for 200 hours (#34)

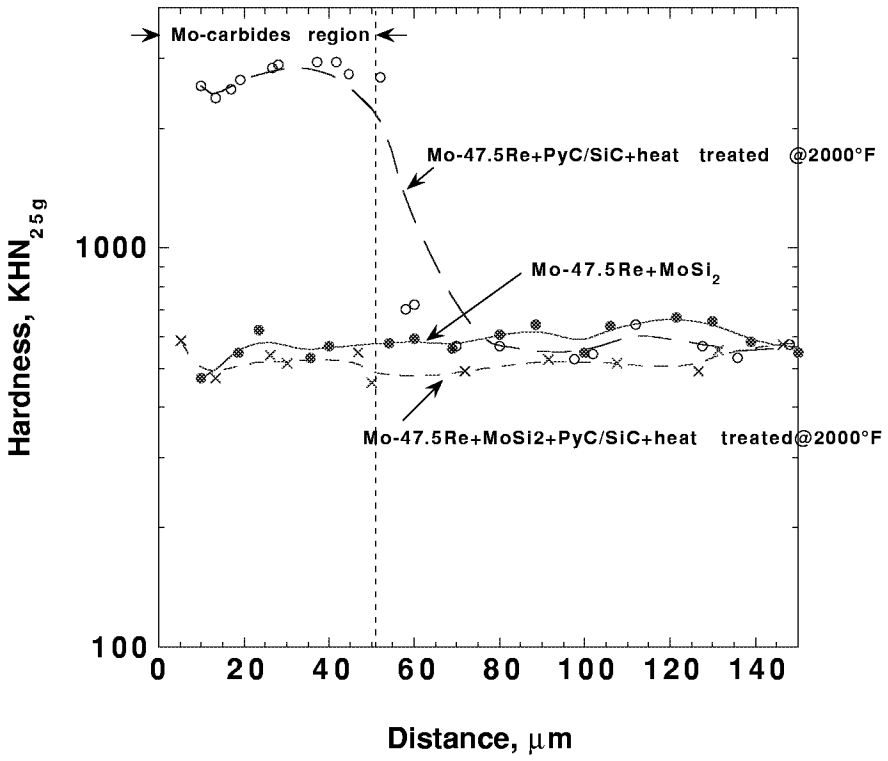

Fig. 15 Hardness depth profiles as a function of depth into the substrate for various conditions of PM Mo-47.5Re.

In the uncoated condition, the hardness of the Mo-47.5Re substrate was 445±35 KHN. Microhardness depth profiles in the substrates for various conditions are presented in Fig. 15. With reference to Fig. 15, it is clear that without a diffusion barrier coating, the 2000°F/200 hr heat treatment produced a 50-60-μm thick, hard, and brittle Mo-carbide layer between the substrate and the PyC/SiC layer. The x-ray elemental maps for this condition are presented in Fig. 16. With respect to the SiK_α map therein, it is evident that ~14-μm thickness of the Mo-Re substrate is affected by Si diffusion. Of this, the first ~6-μm thickness appears to be comprised of a Mo-

silicide layer with a distinct mottled appearance (see the corresponding BSE image), and the remaining 8-μm thickness a Mo-Re-Si solid solution. The presence of the original PyC layer is evidenced by the vertical strip of high carbon intensity on the extreme left side of the CK_α map. The ubiquitous presence of carbon in the CK_α map also attests to substantial carbon diffusion in the Mo-Re substrate as a result of the heat treatment.

In contrast to the uncoated condition, the $MoSi_2$(Ge) barrier coating effectively prevented the Mo-carbide formation. The substrate hardness for the various conditions are plotted as a bar graph in Fig. 17. Even when the sample was $MoSi_2$(Ge) coated with no PyC/SiC deposition, the nominal substrate hardness was substantially higher than the uncoated condition. The elemental x-ray maps for this sample are presented in Fig. 18. The Si x-ray map therein shows a ~10-μm thick Si-depleted region within the original $MoSi_2$(Ge) layer at the coating/substrate interface; no perceivable Si diffusion into the substrate is apparent. The substantial increase in the substrate hardness for this condition is therefore likely to be due to rather copious amounts of the χ (MoRe) phase, brought about by the high-temperature effects associated with the coating process. The presence of the Si-depleted layer within the $MoSi_2$(Ge) layer also implies that $MoSi_2$(Ge) is unstable when it is in contact with the Mo-47.5Re substrate at the coating temperatures. In addition, cracks parallel to the coating/substrate interface were apparent within the coating.

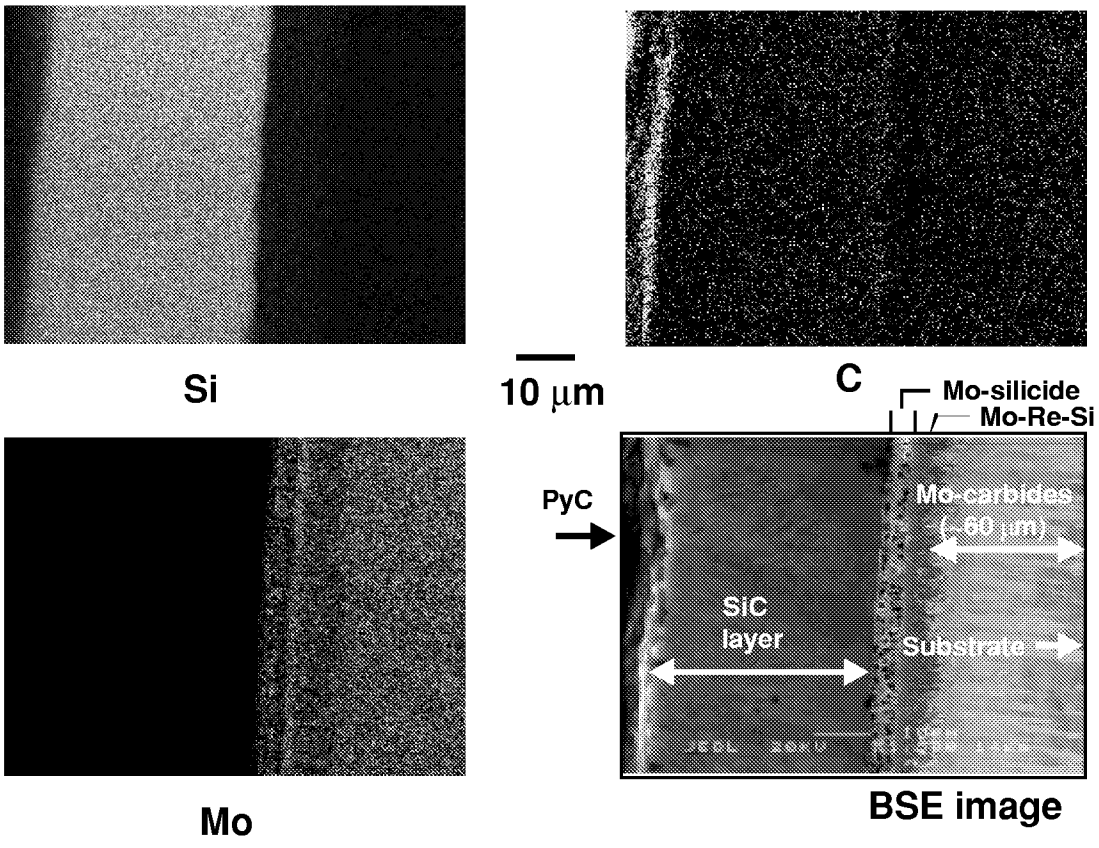

Fig. 16 Elemental x-ray maps for uncoated PM Mo-47.5Re with PyC/SiC deposition and heat treated at 2000°F for 200 hr (#29).

In comparison with the uncoated condition, it is seen that the Mo-47.5Re substrate hardness was markedly higher whenever the samples were embedded in PyC/SiC (and subsequently heat treated) whether they were $MoSi_2$(Ge) coated or not (see Fig. 17). When the tube was embedded in PyC/SiC but not coated, the hardness increase appeared to be related to the diffusion of both

elemental Si and C from PyC/SiC into the substrate. By the same token, when the sample was coated with PyC/SiC subsequent to $MoSi_2$(Ge) coating, the hardness increase stemmed essentially from Si diffusion into the substrate. This is amply demonstrated in Fig. 19, which shows the x-ray maps for the $MoSi_2$(Ge)-coated and the PyC/SiC-embedded sample, subsequent to the 2000°F/200 hr heat treatment. It is clear from this figure that the original 17-μm thick $MoSi_2$(Ge) coating totally disappeared in addition to migration of large amounts of Si away from the PyC/SiC into the substrate. The substrate appeared to be substantially enriched in Si. Also, a ~10-μm thick, freshly formed Mo-silicide layer was observed as shown in Fig. 20.

For the 2000°F/200 hr heat treated condition, Re-rich precipitates formed either at the grain boundaries or within the alloy matrix (see Fig. 20). As per the Mo-Re phase diagram, this alloy was in the two-phase region with (Mo) and χ as the equilibrium phases. (Mo) is a Mo-Re solid solution while the χ phase is an intermetallic with the ReMo composition. The 2000°F/200 hr heat treatment appeared to readily favor the precipitation of the χ phase, thus conforming the alloy to equilibrium conditions of alloy stability. Grain boundary precipitation of intermetallic phases, in general, may have a detrimental effect on eventual ductility properties of the substrate, regardless of whether the substrate is coated or uncoated.

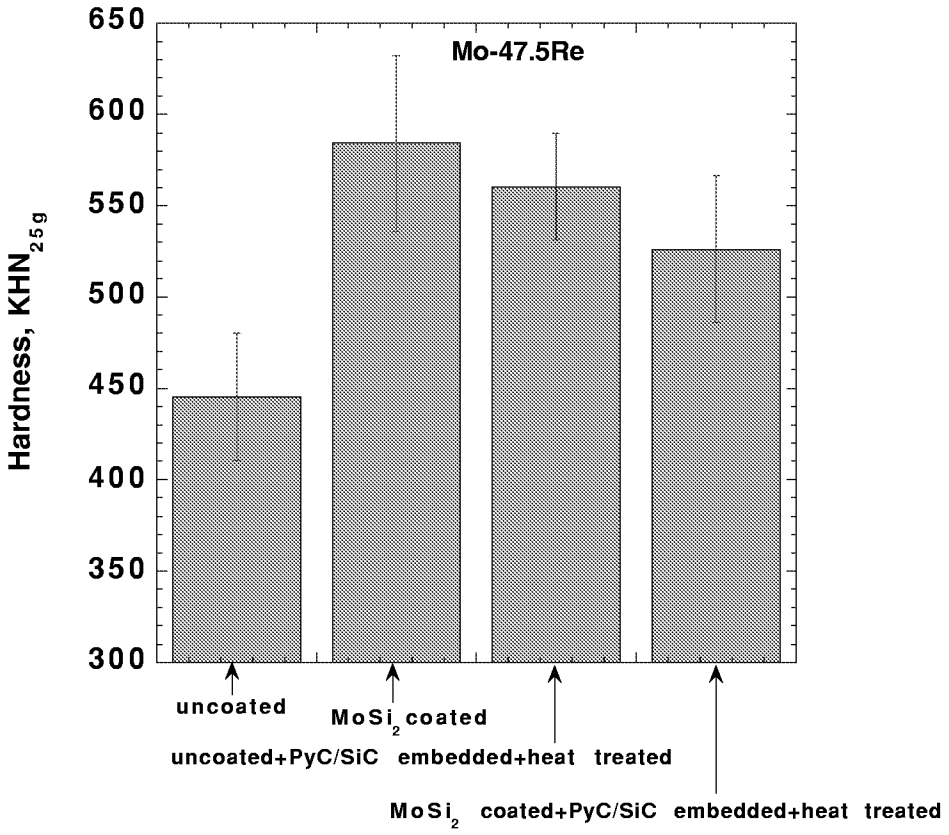

Fig. 17 Substrate hardness of Mo-47.5Re in various conditions.

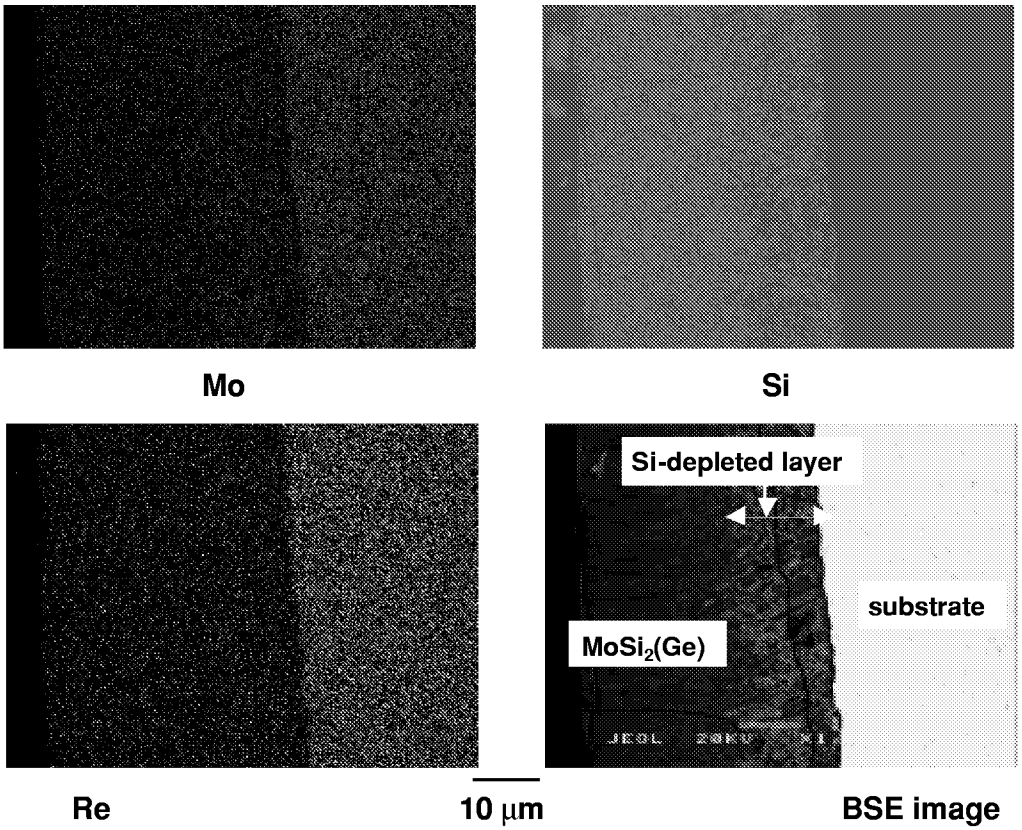

Fig. 18 Elemental x-ray maps for $MoSi_2(Ge)$-coated PM Mo-47.5Re (#2).

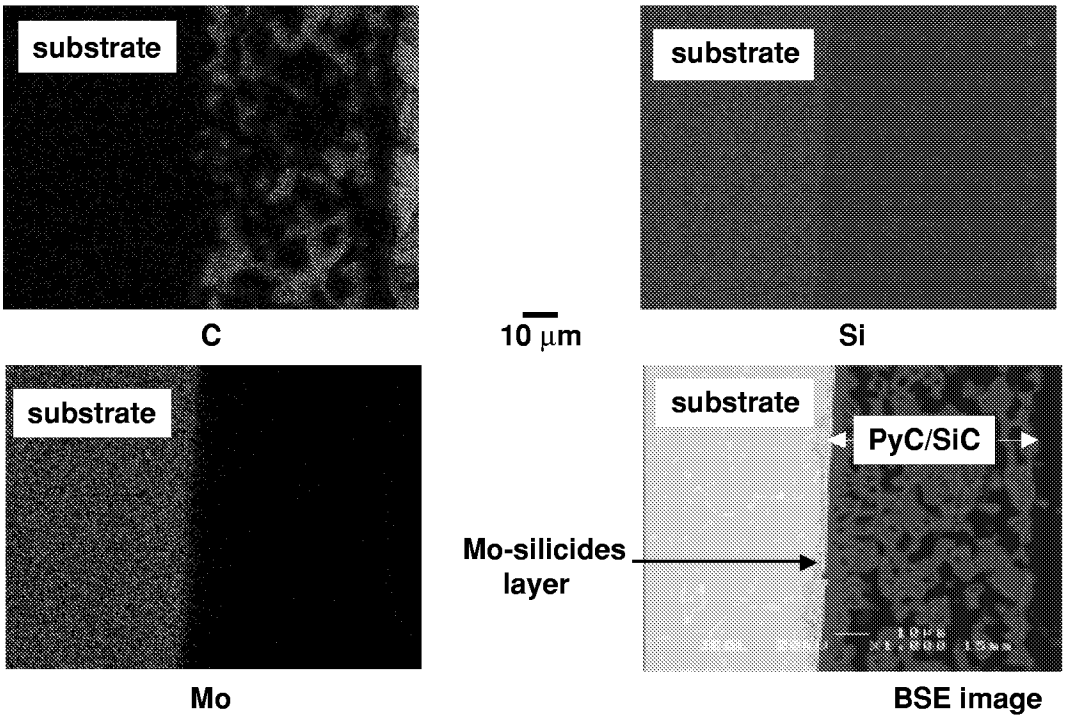

Fig. 19 Elemental x-ray maps for $MoSi_2(Ge)$-coated PM Mo-47.5Re with PyC/SiC deposition and heat treated at 2000°F for 200 hr (#34).

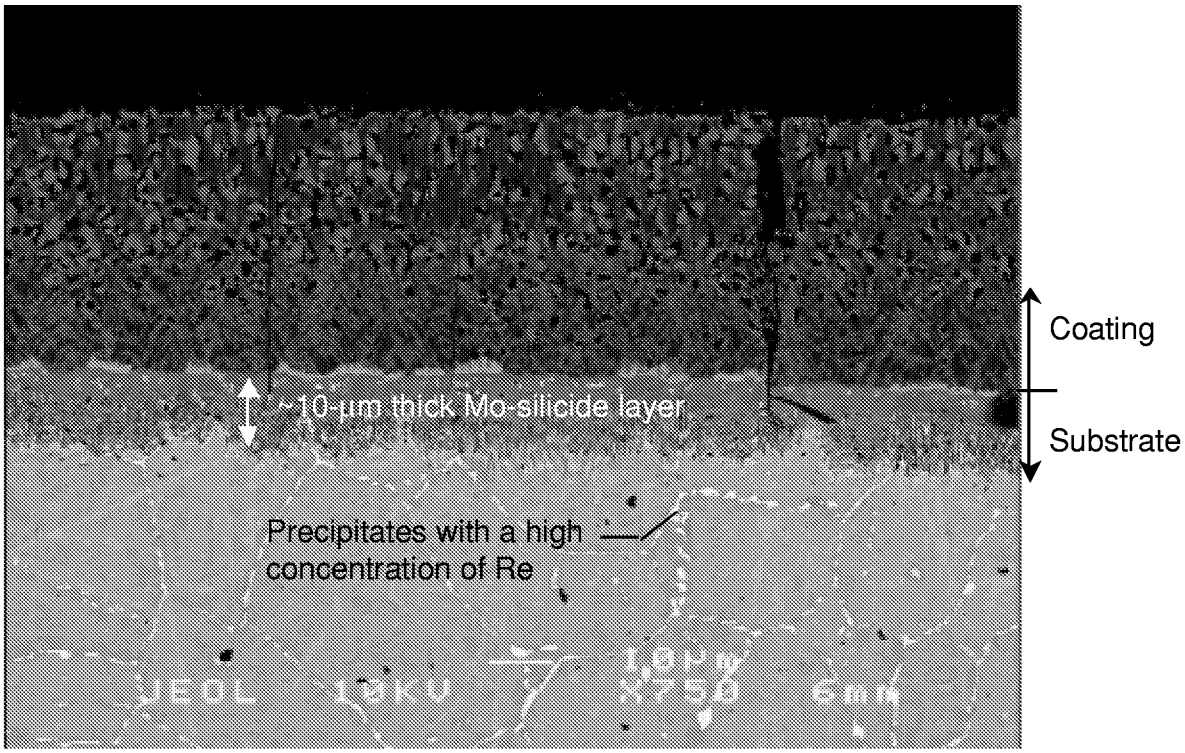

Fig. 20 SEM micrograph of $MoSi_2$(Ge)-coated PM Mo-47.5Re with PyC/SiC deposition and heat treated at 2000°F for 200 hr (#34).

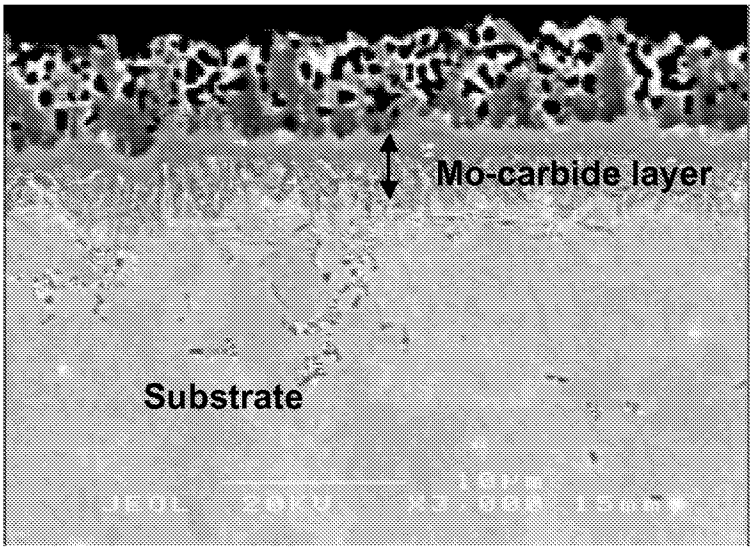

Fig. 21 SEM micrograph of uncoated AC Mo with PyC/SiC deposition (#20).

AC Mo

AC Mo tubes with and without a $MoSi_2$(Ge) coating were characterized in the following conditions.

- Uncoated (#10)
- Uncoated with PyC/SiC deposition (#20)

- $MoSi_2$(Ge) coated (#11)
- $MoSi_2$(Ge) coated with PyC/SiC deposition (#26)
- $MoSi_2$(Ge) coated with PyC/SiC deposition and heat treated at 2000°F for 200 hr (#27)

The BSE image for the uncoated AC Mo sample with PyC/SiC deposition (see Fig. 21) showed that significant levels of porosity existed in the original PyC/SiC layer. Also, a ~5-μm thick Mo-carbide layer is evident in the Mo substrate at the original substrate/PyC/SiC interface. In the AC Mo sample coated with $MoSi_2$(Ge) (see Fig. 22), large transverse cracks are seen in the ~50-μm thick $MoSi_2$(Ge) layer. Minute pores, intrinsic to the coating process, are also evident in this layer. The presence of interdendritic shrinkage cavities in the Mo substrate attests to the metal deficit experienced during solidification, subsequent to the arc casting of the Mo tubes. No interaction products are evident, however, at the substrate/coating interface.

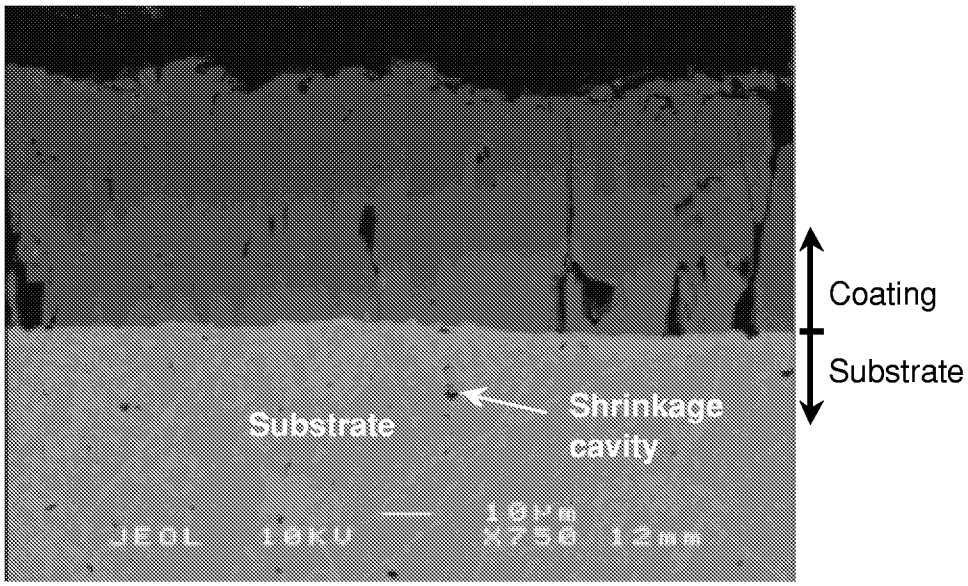

Fig. 22 SEM micrograph of $MoSi_2$(Ge)-coated AC Mo in as coated condition (#11).

The SEM image together with the x-ray elemental maps for Si, C, and Mo are presented in Fig. 23 for the $MoSi_2$(Ge)-coated sample with PyC/SiC deposition. Note that for this condition, a ~10-μm thick Mo-silicide layer is present at the substrate/coating interface. No Mo-carbide layer developed in the substrate, however. Large transverse cracks appear to traverse the entire thickness comprising the PyC/SiC + Mo-silicides layers, thus compromising its mechanical integrity. From the CKα map it is apparent that these cracks served as paths for C diffusion into the substrate through the intervening SiC layer of the PyC/SiC deposition layer. With respect to the MoK_α map, it is clear that the PyC/SiC deposition layer is contaminated with Mo. The original $MoSi_2$(Ge) layer in contact with the PyC/SiC deposition may therefore not be fully chemically stable. This may result in part of the $MoSi_2$ disintegrating into Mo and Si. Mo may migrate to the PyC/SiC layer while Si may diffuse into the Mo substrate. From the SiK_α map, a minute amount of Si appears to have diffused into the substrate. Subsequent to the 2000°F/200 hr heat treatment (see Fig. 24), the transverse cracks formed within the original PyC/SiC layer appear to be wider together with a thicker (~20 μm) Mo-silicide layer formation at the original substrate/$MoSi_2$(Ge) interface. A thicker Mo-silicide layer in the 2000°F/200 hr heat treated condition compared to that in the un-heat treated condition suggests that the prolonged heat treatment promoted further deterioration of the SiC layer, and the chemical reaction of Si with the Mo substrate. Furthermore, a mild Mo enrichment of the SiC layer is also apparent. The CKα elemental map once again indicates that C from PyC diffused through the transverse cracks into the Mo substrate thereby promoting the

formation of a Mo-C solid solution layer in the substrate. The 2000°F/200 hr heat treatment thus had an adverse effect on the overall physical and chemical stabilities of both the coatings and the substrate.

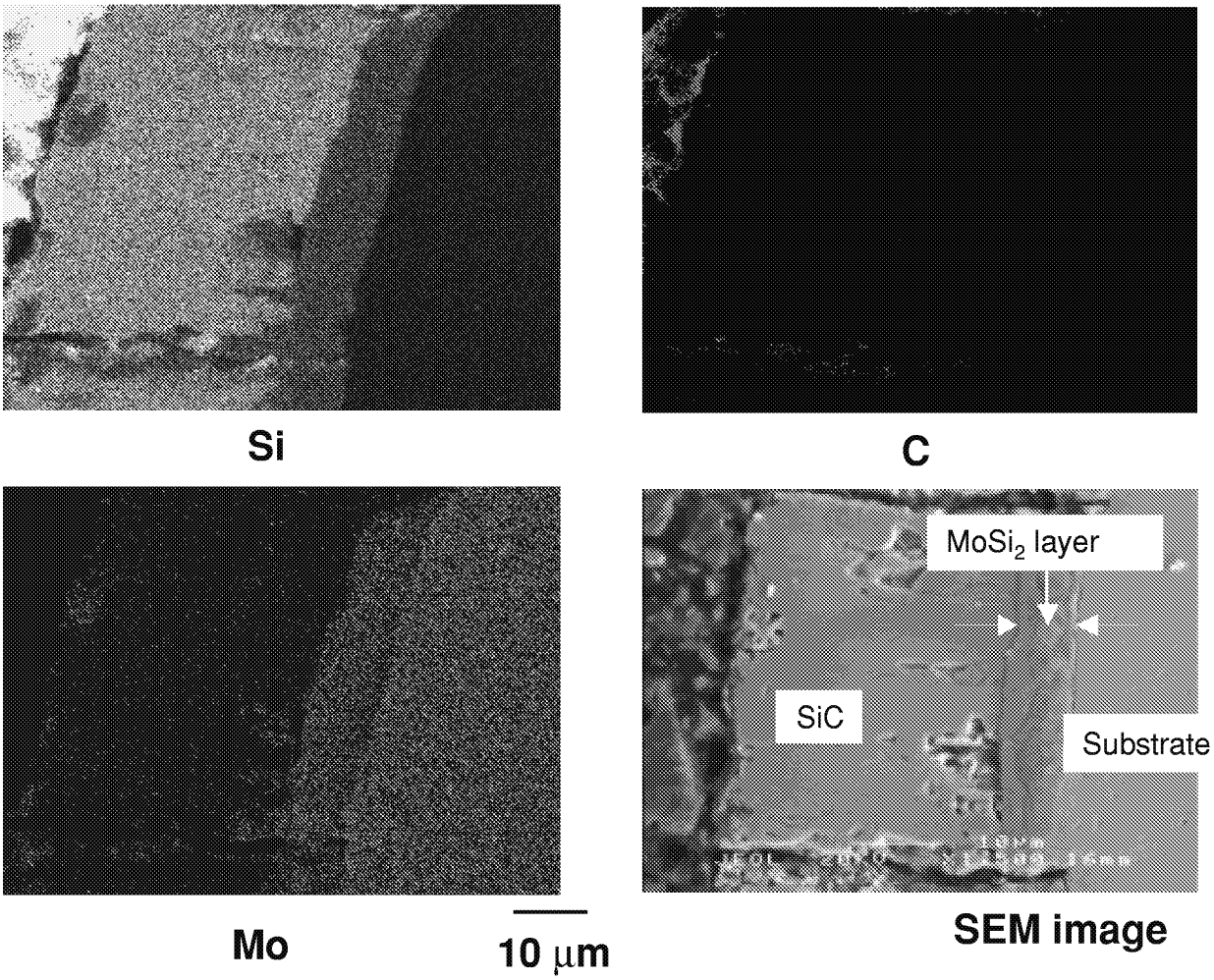

Fig. 23 Elemental x-ray maps for $MoSi_2$(Ge)-coated AC Mo with PyC/SiC deposition in the as coated condition (#26).

Nominal hardness variations for different conditions of the Mo substrate are presented in Fig. 25. With respect to the uncoated condition, the hardness of the $MoSi_2$(Ge) coated substrate was significantly lower, indicating possible softening of the substrate due to high-temperature effects associated with the coating process. Subsequent to the deposition of PyC/SiC (deposition temperature of ~ 2000°F) and the further heat treatment at 2000°F for 200 hours, the substrate hardness increased, possibly due to minor alloying with C and/or Si. The CKα x-ray map in Fig. 24 does indicate a mild contamination of the substrate through C diffusion. The hardness data thus appear to be sensitive enough to show minor changes in substrate chemistry.

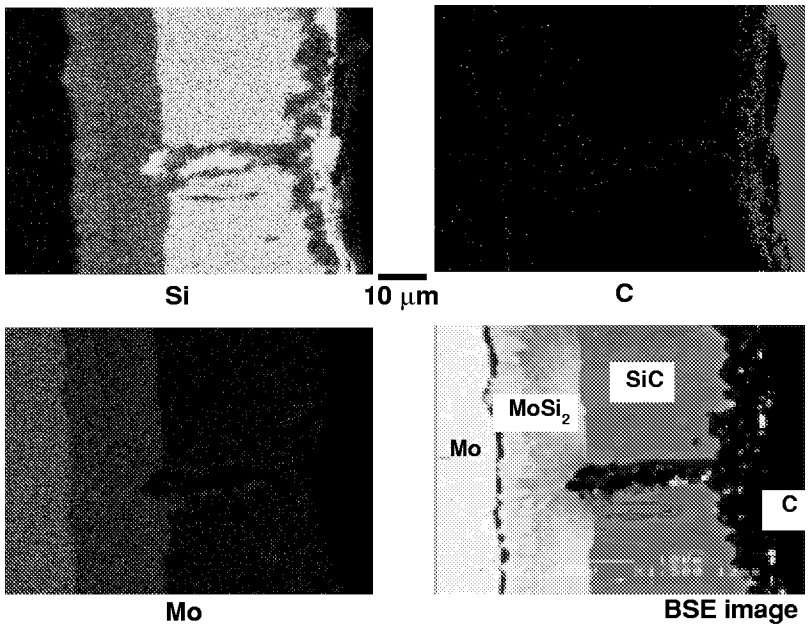

Fig. 24 Elemental x-ray maps of $MoSi_2$(Ge)-coated AC Mo with PyC/SiC deposition heat treated at 2000°F/200 hr (#27).

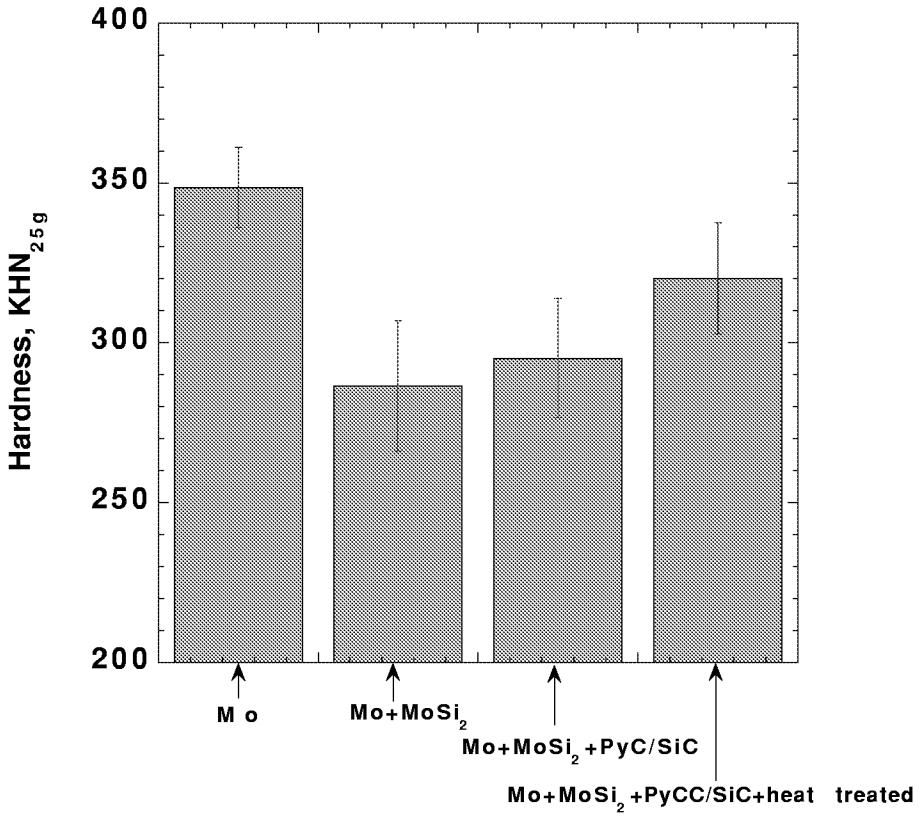

Fig. 25 Substrate hardness of AC Mo in various conditions.

TiB_2 Coating

Samples of arc cast Mo and PM Mo-47.5Re were coated with a TiB_2 coating using the CVD process. The coatings were applied by the Applied Technology Coatings (ATC), Fort Worth, TX.

AC Mo

Samples of AC Mo, with and without TiB_2 coating, were characterized in the following conditions:

- Uncoated (#10)
- Uncoated with PyC/SiC deposition (#20)
- TiB_2 coated (#4)
- TiB_2 coated with PyC/SiC deposition (#24)
- TiB_2 coated with PyC/SiC deposition and heat treated at 2000°F for 200 hr (#30)

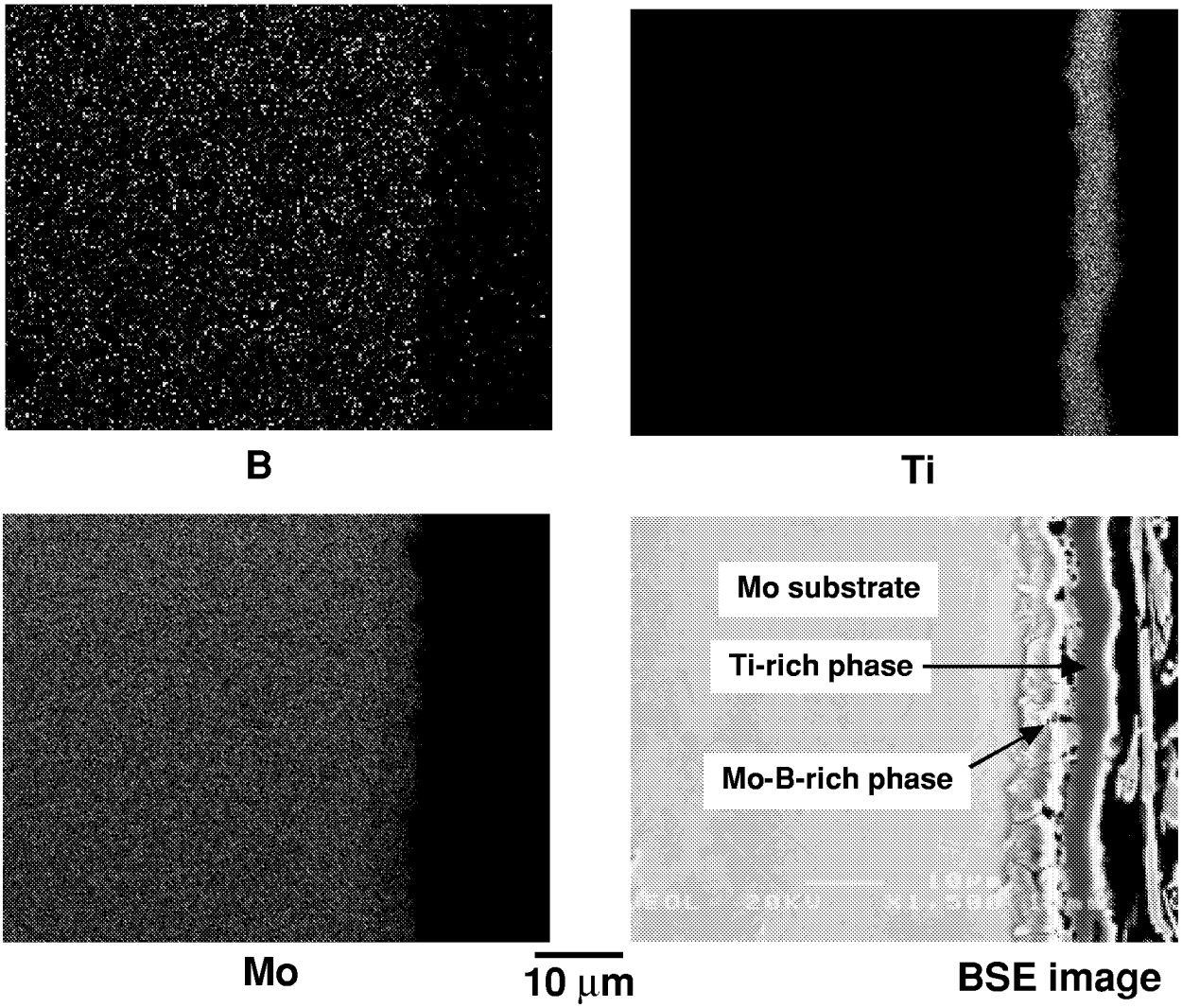

Fig. 26 X-ray elemental maps for TiB_2–coated AC Mo in the as-coated condition (#4).

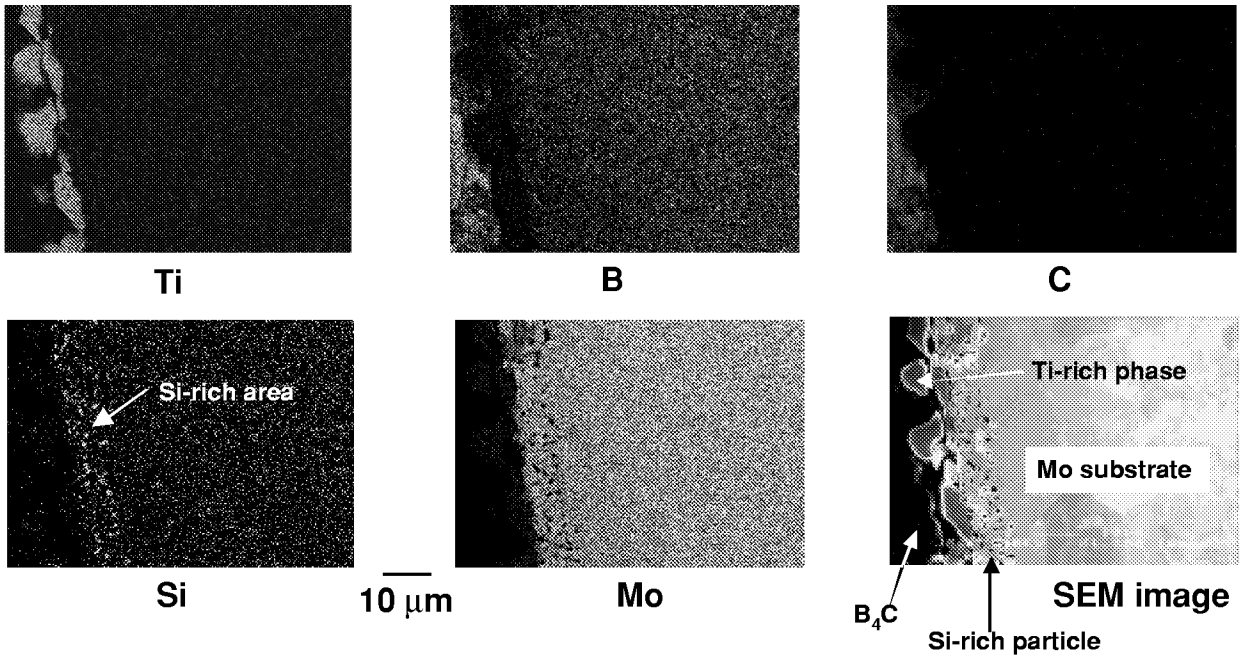

Fig. 27 X-ray elemental maps for TiB_2-coated AC Mo with PyC/SiC heat treated at 2000°F for 200 hr (#30).

The effects of the TiB_2 coating on Mo may be summarized by Fig. 26 and Fig. 27. From Fig. 26, it is clear that the TiB_2 coating was chemically unstable in contact with the Mo substrate at the coating temperature and below. The site of the original TiB_2 coating was replaced by a Ti-rich layer, which was largely depleted in B. Furthermore, a thin layer of a Mo-B-rich phase is apparent at the substrate/coating interface. With reference to the binary Mo-B phase diagram, the possible Mo-B-rich phases for increasing B concentrations are Mo_2B, αMoB, Mo_2B_5 or MoB_4, respectively. Subsequent to PyC/SiC deposition followed by the 2000°F/200 hr heat treatment, the chemistries of the coating/substrate were further altered drastically as shown in Fig. 27. The one-to-one correspondence in the B and the C elemental maps suggests a strong affinity for B in the TiB_2 coating with C in the PyC/SiC deposition. In addition, a thin layer of Si-rich particles with a mottled appearance is seen at the coating/substrate interface. This layer is perhaps comprised of Mo-silicide particles. Thus, it is clear that TiB_2 as a coating material for Mo suffered from severe chemical incompatibility problems.

PM Mo-47.5Re

PM Mo-47.5Re with and without the TiB_2 coating was characterized in the following conditions:

- Uncoated (#3)
- Uncoated with PyC/SiC deposition (#28)
- Uncoated with PyC/SiC deposition and heat treated at 2000°F for 200 hr (#29)
- TiB_2 coated (#1)
- TiB_2 coated with PyC/SiC deposition (#25)
- TiB_2 coated with PyC/SiC deposition and heat treated at 2000°F for 200 hr (#35)

Just as in AC Mo-41Re and AC Mo with no diffusion barrier coating, a Mo-carbide layer was also apparent in the uncoated PM Mo-47.5Re samples that were embedded in PyC/SiC. This condition is not further discussed here since it was discussed previously.

The TiB_2-coated condition (#1) was distinguished by a smooth TiB_2/substrate interface and a coating thickness of ~30 μm (with a hardness of ~4800±340 KHN). A few transverse cracks were also apparent in the coating. The Mo-47.5Re substrate showed 10-15-μm wide grains. Some of the grains contained fine-sized Re-rich precipitates (probably the χ(ReMo) phase). EDS spectra indicated that B from the TiB_2 coating diffused into the substrate to a depth of ~15 μm even during the process of coating with TiB_2. The x-ray elemental maps for this condition are presented in Fig. 28. With reference to this figure, it is pertinent to note that unlike the TiB_2-coated Mo, the TiB_2-coated Mo-47.5Re alloy was substantially more stable and also distinguished by the absence of Mo-B-rich phases at the coating/substrate interface. In contrast to unalloyed Mo, the presence of 47.5%Re in Mo thus appeared to confer superior chemical stability on the alloy vis-à-vis the TiB_2 coating.

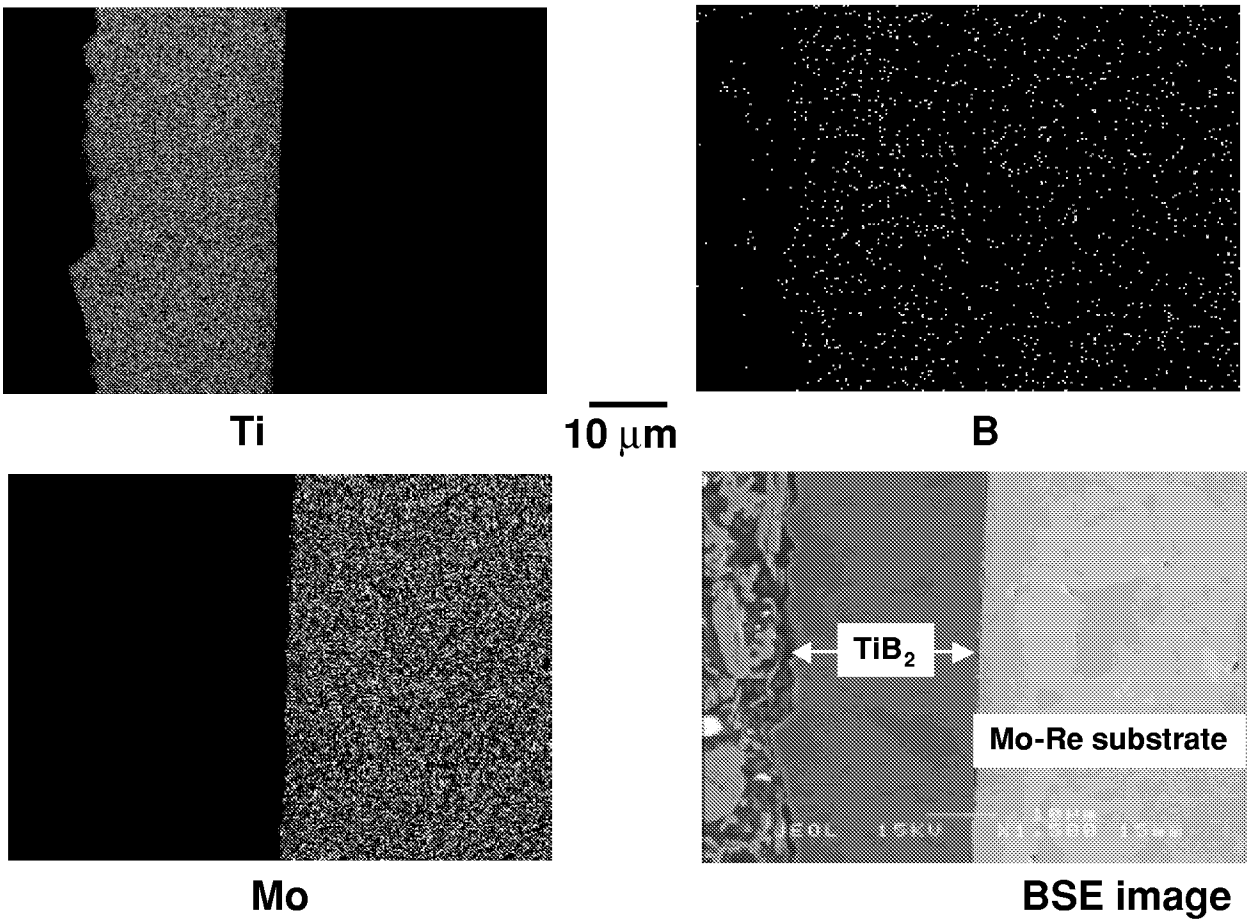

Fig. 28 X-ray elemental maps for TiB_2–coated PM Mo-47.5Re (#1).

Changes in the chemistries of the Mo-47.5Re substrate, the original TiB_2 coating, and the PyC/SiC deposition, consequent to the 2000°F/200 hr heat treatment are shown in Fig. 29, with the substrate on the left side of each image. In the region of the TiB_2 and PyC/SiC layers, the x-ray maps of B and C correspond to each other on a one-to-one basis. This implies that a significant amount of B from the original TiB_2 coating combined with C from the PyC/SiC deposition to form boron carbide (perhaps B_4C). The presence of boron carbide is apparent throughout the TiB_2 and PyC/SiC layer. From the B-C binary phase diagram, formation of B_4C needs at least 9.8 wt.% C and this appeared to be readily available from PyC/SiC during the 2000°F/200 hr heat treatment. The substrate enrichment with B (as indicated by the B x-ray map) accounted for the rest of the boron in the original TiB_2 layer. The corresponding x-ray map for Ti and the BSE image clearly

indicate the B_4C regions formed islands within the network of Ti-rich regions. The Si x-ray map together with the BSE image indicate that Si from SiC (in PyC/SiC) not only formed a ~10-μm-thick Mo-silicide layer in the substrate at the substrate/coating interface, but also diffused appreciably into the substrate. The dispersion of both B and Si from the composite layer of TiB_2 and PyC/SiC into the substrate thus implies severe chemical instabilities for both TiB_2 and the PyC/SiC in the presence of each other and hence the inadequacy of TiB_2 as a protective barrier. Although TiB_2 appears to have succeeded in preventing Mo-carbides formation, the significant problem of inherent incompatibility between TiB_2 and PyC/SiC still exists.

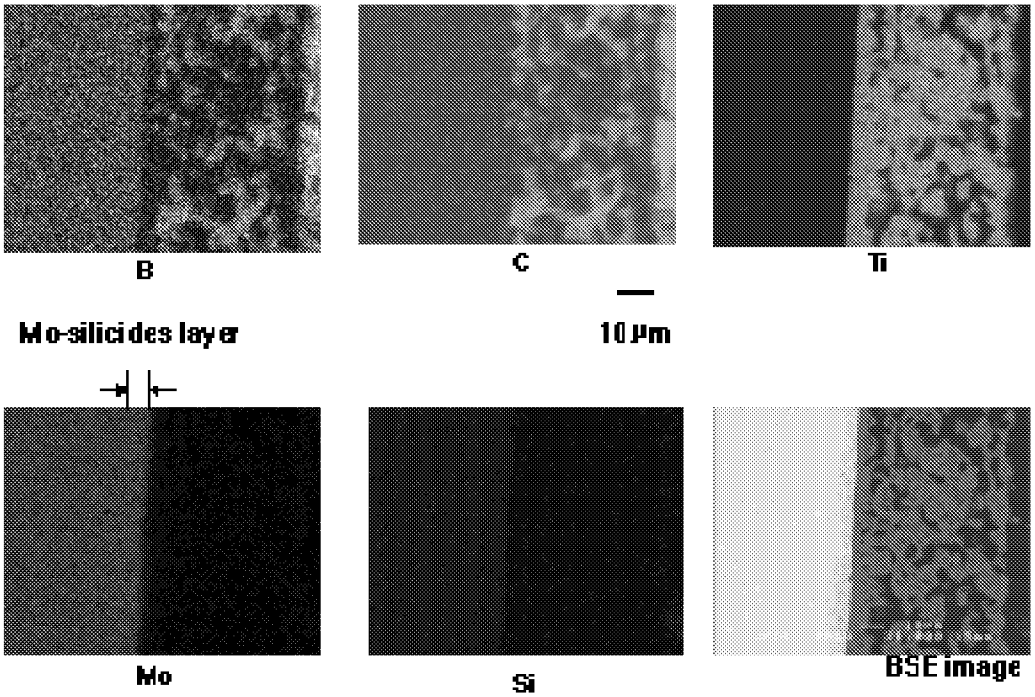

Fig. 29 Elemental x-ray maps in TiB_2-coated PM Mo-47.5Re with PyC/SiC deposition and heat treated at 2000°F for 200 hr (#35).

In the uncoated condition, the Mo-47.5Re substrate had an average hardness number of 445±35 KHN. In the TiB_2-coated condition, the substrate had a moderately elevated hardness of 467±38 KHN, with no evidence of an interface reaction product layer consequent to the coating process. However, a mild hardness gradient with respect to the coating/substrate interface was observed in the substrate. The presence of a mild hardness gradient together with an observed increase in the substrate hardness for the coated condition implies that B from the TiB_2 may have diffused into the substrate. Subsequent to PyC/SiC deposition, followed by the 2000°F/200 hr heat treatment (#35), the substrate hardness increased appreciably. With reference to Fig. 29, it is clear that for this alloy condition, significant levels of B (from TiB_2 coating) and Si (from PyC/SiC deposition) were present in the substrate, thus rendering it harder. The substrate hardness values for the various conditions are represented in Fig. 30.

The following general observations may be made with regard to the influence of chemistry differences in Mo-Re alloys on precipitate microstructures, as predicated by heat treatments. In the Mo-47.5Re alloy sample subjected to the 2000°F/200 hr heat treatment (in contrast to the Mo-41Re alloy heat treated in the same manner), regardless of whether the alloy was coated with either TiB_2 or $MoSi_2$(Ge), Re-rich precipitates formed both within the alloy and at grain boundaries. Based on the Mo-Re equilibrium phase diagram, the 47.5%Re alloy (unlike the Mo-41Re which was

essentially a single phase solid solution of Mo and Re) was in the two phase region, (Mo) + χ. The 2000°F/200 hr heat treatment likely hastened the precipitation of equlibrium amount of the χ(ReMo) phase. Grain boundary precipitation of these intermetallic precipitates may have detrimental effects on strength and ductility of the substrate. The substantial increase in the substrate hardness of the TiB_2 coated with PyC/SiC deposition and heat treatment (see Fig. 30) may be a result of appreciable levels of B, and also the χ precipitates present in the substrate. This observation once again points to inherent instability of the TiB_2 coating and also the potential degrading influence of the χ precipitates on the ductility properties of the substrate.

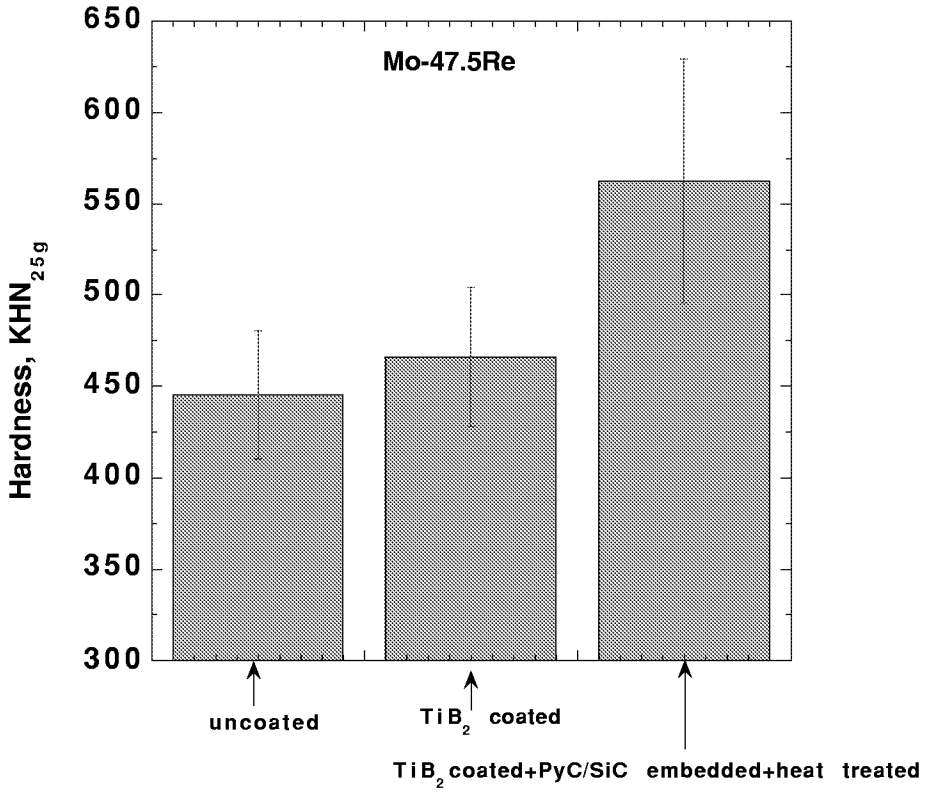

Fig. 30 Variation in substrate hardness of PM Mo-47.5Re.

Burst Tests

Burst tests were performed on several of the refractory-metal tubes with and without diffusion barrier coatings, and prior to and after PyC and SiC deposition by the simulated HACI C/SiC process. The tubes were taken through the entire HACI deposition process, but were not embedded in a carbon fiber preform. Due to nonavailability of samples, burst tests on tubes embedded in C/C were not conducted.

The tubes were burst tested at room temperature using pressurized water. Swage lock fittings were used to seal the tubes at each end. In several cases, the tube diameters were not standard, and the fittings had to be drilled out to fit the tubes. During testing, the pressure was increased in ~250 psi intervals every 30 sec. There were no long hold times at any pressure. Fig. 31 shows photographs of the test setup and a Mo-Re tube both a) before and b) after burst testing. An

attempt was made to test tube lengths greater than several diameters, but that was not always possible.

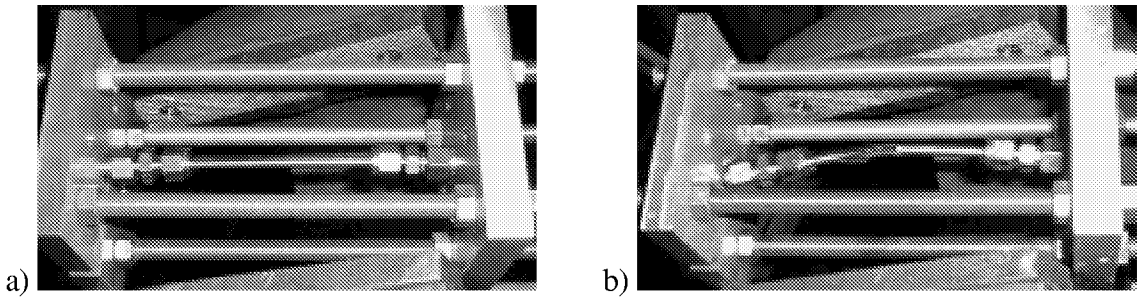

Fig. 31 Photograph of the test apparatus and tube, a) prior to and, b) after burst testing.

The results of the burst tests are shown in Table 2. The specimen number, diffusion barrier coating (if any), environment (PyC/SiC processing), time at temperature excluding coating and processing exposure, burst pressure, and failure stress are shown in the table for each tube material. The outer diameter (OD) and inner diameter (ID) are also given for each tube. In all cases, the failure stress, σ, was calculated from

$$\sigma = P\, r / t$$

where P is the burst pressure, r is the average of the inner and outer radii of the tube, and t is the tube wall thickness. In the measurement of r, contribution to thickness included any protective coating such as TiB_2 and $MoSi_2$(Ge), as well as the PyC/SiC deposition. Several of the tubes broke during handling and were not tested; while during other tests, fittings leaked or failed during testing thus limiting the pressures attained. For cases where the tube did not burst, the burst pressure and failure stress are listed in Table 2 preceded by ">". For each test condition, only one tube was tested. Thus, the burst strength evaluation may be considered exploratory and no claims to statistical significance are made.

The PM Mo-47.5Re tubes provided the most complete burst test data. These tubes were tested in the uncoated and coated (TiB_2 and $MoSi_2$(Ge)) conditions both before and after the PyC/SiC deposition. All of the tube lengths (distance between sleeve on fittings) were greater than 1 in. except for specimen #23 (0.603-in. long), specimen #25 (0.188-in. long), and specimen #29 (0.605 in.). From the burst test data, there appears to be a slight degradation in the tube strength due to the application of the TiB_2 and $MoSi_2$(Ge) coatings. In addition, the PyC/SiC deposition process appeared to degrade the strength of each of the tubes. However, the uncoated tube strength was only reduced 8.7% by the PyC/SiC deposition, versus strength reduction of 17.2% for the $MoSi_2$(Ge) barrier coating and 22.5% for the TiB_2 barrier coating. For the uncoated tube with PyC/SiC processing, exposure at 2000°F for 200 hours reduced the burst strength only slightly from the as-processed state.

The AC Mo-41Re tubes had a 0.030-in. wall thickness, and required large pressures to burst. As a result, in some cases the burst pressure exceeded the test capability. The length of the AC Mo-41Re tubes were 0.99 in. for specimen #12, 0.986 in. for specimen #13, 0.394 in. for specimen #14, and 0.658 in. for specimen #15. Due to testing limitations, specimens #12, #13, and #14 did not burst. However, an increase in diameter of 0.001 in. was measured after the tests. Specimen #15, which was an AC Mo-41Re tube with a $MoSi_2$(Ge) coating, failed at approximately 130 ksi. The burst strength of specimen #16, which also included exposure at 2000°F for 200 hours, was significantly degraded versus the as-processed condition (#15). Though it was difficult to isolate the contributions of tube material processing (AC versus PM) and chemistry (41%Re versus

47.5%Re) on the AC and PM tube strengths, it did appear that the AC tubes were significantly stronger than the PM tubes.

Table 2. Results of Burst Tests

Spec. No.	Coating, environment, and thermal exposure	Burst pressure, psi	Failure stress, ksi
PM Mo-47.5Re, OD = 0.197 in., ID = 0.175 in.			
3	uncoated	11,509	97.3
28	PyC/SiC	10,507	88.8
29	PyC/SiC and 200 hr at 2000°F	10,200	86.2
1	TiB_2	11,073	93.6
25	TiB_2, PyC/SiC	8,577	72.5
2	$MoSi_2$(Ge)	11,315	95.7
23	$MoSi_2$(Ge), PyC/SiC	9,368	79.2
AC Mo-41Re, OD = 0.188 in., ID = 0.128 in.			
12	uncoated	> 60,700	> 158
14	PyC/SiC	> 48,000	> 126.4
13	$MoSi_2$(Ge)	> 47,300	> 124.5
15	$MoSi_2$(Ge), PyC/SiC	49,500	130.3
16	$MoSi_2$(Ge), PyC/SiC and 200 hr at 2000°F	42,000	110.6
CVD Re, OD = 0.195 in., ID = 0.185 in.			
6	uncoated	> 5946	> 113
18	PyC/SiC	broke prior to testing	
CVD Nb, OD = 0.204 in., ID = 0.186 in.			
7	uncoated	2101	22.8
19	PyC/SiC	broke prior to testing	
AC Mo, OD = 0.188 in., ID = 0.137 in.			
20	PyC/SiC	15,565	49.6

The uncoated CVD Re tube withstood a stress of 113 ksi without failure while the uncoated CVD Nb tube failed at a stress of 22.8 ksi. Both the Re and Nb tubes with the PyC/SiC deposition broke prior to testing, and hence no meaningful trends could be established. The burst stress of 49.6 ksi is significantly below the ultimate of 109 ksi for Mo, indicating that the Mo was detrimentally affected by the PyC/SiC deposition. In the case of the Re, Nb, and Mo burst test specimens, only a single datum point was available, and therefore a comparison of the different conditions is not possible.

Despite the limited number of conditions evaluated and the lack of replicates, the burst test data indicated the following:

- Although the effects of the barrier coatings and PyC/SiC deposition on the AC Mo-41Re could not be determined fully due to testing limitations, the $MoSi_2$(Ge) coating appeared to substantially degrade the burst strength relative to the uncoated condition.
- Both TiB_2 and $MoSi_2$(Ge) coatings followed by a PyC/SiC deposition, moderately degraded the burst strength of PM Mo-47.5Re relative to uncoated PM Mo-47.5Re.
- AC Mo-41Re appeared to be significantly stronger than PM Mo-47.5Re.

Concluding Remarks

Metallurgical characterization (microhardness survey and SEM examination) and burst tests were performed on several different refractory metals and alloys, with the major effort directed toward Mo and Mo-Re alloys. The following observations can be made:

- For the PM Mo-47.5Re alloy, burst strength degraded moderately when the alloy tubes were coated with either $MoSi_2$(Ge) or TiB_2 (relative to the uncoated condition). The degradation in burst strength was more drastic subsequent to the coating followed by the PyC/SiC deposition, with contribution to degradation from TiB_2 being more severe than from $MoSi_2$(Ge). $MoSi_2$(Ge) thus appears to be more effective than TiB_2 as a protective barrier coating for PM Mo-47.5Re.

- The AC Mo-41Re alloy appears to have significantly higher burst strength (though not enough samples were available for a statically significant test) than the PM Mo-47.5Re alloy, when the comparisons are made with respect to uncoated, $MoSi_2$(Ge) coated, PyC/SiC deposited, or $MoSi_2$ coated + PyC/SiC deposited conditions. Mo-41Re is essentially a single phase alloy whereas Mo-47.5Re is a two phase alloy. The presence of an appreciable volume fraction of the χ(ReMo) phase at the grain boundaries appeared to be a ductility degrading factor, and may explain the poorer burst strength of PM Mo-47.5Re compared to Mo-41Re.

- The lamellar morphology of the carbide layer evident in the AC Mo-41Re processed with C/C, implies that more than 5.7 wt.% C reacted with Mo (in the Mo-Re substrate) to yield a eutectoid mixture of αMo_2C and MoC. This Mo-carbide layer was hard and brittle, and may severely degrade burst strength.

- The Fe, Si, Cr-rich R512E coating, sandwiched between the Mo-41Re substrate and the C/C layer, very effectively prevented formation of Mo-carbides in the substrate. A Mo-silicide layer formed in the substrate, however, due to the substrate-coating interactions. This silicide layer, though slower growing than the carbide layer (in the uncoated condition), did increase in thickness with heat treatment time, thereby degrading the useful engineering cross-section of the Mo-Re substrate. The development of lateral and transverse cracks in the original R512E coating may diminish the efficacy of the coating.

- Even though coatings seemed to reduce carbide formation, they did so with the creation of a thin silicide layer which seemed to be detrimental to the burst strength.

- TiB_2 was inherently unstable when it was in contact with the Mo substrate, with B possibly tending to form the Mo_2B phase at the coating/substrate interface. In contrast, TiB_2 appeared to be substantially more stable in contact with the Mo-47.5Re substrate.

Acknowledgements

The authors would like to thank the Metals and Thermal Structures Branch at NASA Langley Research Center for funding this work under Contract No. NAS1-96014. The valuable assistance of Mr. Jim Baughman of Analytical Services & Materials, Inc. in the SEM studies of the investigation and Honeywell Advanced Composites, Inc. in the PyC and SiC deposition is gratefully acknowledged.

References

1. Glass, D. E., Camarda, C. J., Merrigan, M. A., and Sena, J. T., "Fabrication and Testing of Mo-Re Heat Pipes Embedded in Carbon/Carbon," *Journal of Spacecraft and Rockets*, Vol. 36, No. 1, 1999, pp. 79-86.

2. Zanner, F. J., Hammetter, W. F., Gronager, J. E., Averill, W. A., and Feber, R. C., "Compatibility of Refractory Metals with Sodium in the Presence of Oxygen and UO2," Sandia Report, SAND85-0850, May 1985.

3. DiStefano, J. R., "Review of Alkali Metal and Refractory Alloy Compatibility for Rankine Cycle Applications," Journal Materials Engineering, Vol. 11, No. 3, 1989, pp. 215-225.

4. Hansen, M., and Anderko, K., "Constitution of Binary Alloys," Metallurgy and Metallurgical Engineering Series, 1958.

5. Askill, J., "Tracer Diffusion Data for Metals, Alloys, and Simple Oxides," IFI/Plenum, New York, 1970.

6. Anon, "Final Report, Wing Leading Edge Heat Pipe Development," Prepared for General Dynamics Corporation, Fort Worth, TX, by Thermacore, Inc., Lancaster, PA, May 16, 1991.

7. Sherman, A. J., Tuffias, R. H., and Kaplan, R. B., "The Properties and Applications of Rhenium Produced by CVD," JOM, The Journal of the Minerals, Metals, and Materials Society, July, 1991, pp. 20-23.

8. Lundberg, Lynn B., "Silicon Carbide - Tungsten Heat Pipes for High-Temperature Service," I&EC Product Research and Development, Vol. 19, June 1980, pp. 241-244.

9. Ranken, W. A., and Lundberg, L. B., "High Temperature Heat Pipes for Terrestrial Applications," AIAA Third International Heat Pipe Conference, Palo Alto, CA, May 22-24, 1978, pp. 283-291.

10. Keddy, E. S., and Ranken, W. A., "Ceramic Heat Pipes for High Temperature Heat Removal" Los Alamos National Laboratory, Los Alamos, NM. Paper No. LA-UR-79-332, ASME 18th National Heat Transfer Conference, San Diego, CA, August 5-8, 1978.

11. Merrigan, M. A., and Keddy, E. S., "High-Temperature Heat Pipes for Waste-Heat Recovery," AIAA Journal of Energy, Vol. 6, No. 5, October 1982.

12. Rovang, Richard D., Hunt, Maribeth E., Dirling, Ray B., Jr., and Holzl, Robert A., "SP-100 High-Temperature Advanced Radiator Development," Proceedings of the Eighth Symposium of Space Nuclear Power Systems, American Institute of Physics, January 6-10, 1991, pp. 702-707.

13. Rovang, R. D., Dirling, R. B., and Holzl, R. A., "Carbon-Carbon Heat Pipe Development for SP-100 Advanced Radiator Concepts," 27th ASME/AIChE/ANS Heat Transfer Conference, Minneapolis, MN, July 28-31, 1991.

14. Yaney, D. L., and Joshi, A., "Reaction Between Niobium and Silicon Carbide at 1373 K," Journal of Materials Research, Vol. 5, No. 10, Oct. 1990, pp. 2197-2208.

15. Joshi, A., Hu, H. S., Jesion, L., Stephens, J. J., and Wadsworth, J., "High-Temperature Interactions of Refractory Metal Matrices with Selected Ceramic Reinforcements," Metallurgical Transactions A, Vol. 21A, November 1990, pp. 2829-2837.

16. Fries, R. J., Cummings, J. E., Hoffman, C. G., and Daily, S. A., "The Chemical Diffusion of Carbon in the Group VIb Metal Carbides," Included in High Temperature Materials, Proceedings of the Sixth Plansee Seminar, Reutte, Austria, June 24-28, 1968.

17. Reagan, P., Miskolczy, G., and Huffman, F., "Development of a CVD Silicon-Carbide-Graphite-Tungsten Heat Pipe Structure," AIAA 16th Thermophysics Conference, Palo Alto, CA, June 23-25, 1981, AIAA Paper 81-1160.

18. Goodale, Douglass, Reagan, Peter, Lieb, David, and Huffman, Fred, "Thermionic Converters for Terrestrial Applications," Thermo Electron Corp., Waltham, MA, Proceedings of the 17th Intersociety Energy Conversion Engineering Conference, Aug. 8-12, 1982, pp. 1913-1917.

19. Hartenstine, John R., and Henson, Thomas P., "The Development of Carbon-Carbon Vacuum Envelopes for Hypersonic Vehicle Heat Pipe Applications," SBIR Phase I Report, June 1991, Wright-Patterson AFB, Contract No. F33657-90-C-2207.

20. Rabin, B. H., "A Review of Silicon Carbide/Metal Interactions with Relevance to Silicon Carbide Joining," EGG-MS-9633, Prepared for the Office of Fossil Energy, U.S. Department of Energy, Idaho Operations Office, DOE Contract No. DE-AC07-76ID01570, 1991.

21. Isobe, Y., Son, P., and Miyake, M., "Carbide Layer Growth Behavior in a Molybdenum Coating on Graphite at Elevated Temperatures," Journal of the Less-Common Metals, Vol. 147, 1989, pp. 261-268.

22. Tortorici, P. C., and Dayananda, M. A., "Growth of Silicides and Interdiffusion on the Mo-Si System," Metallurgical and Materials Transactions A, Vol. 30A, 1999, pp. 545-550.

23. Martinelli, A. E., Drew, R. A. L., and Berriche, R., "Correlation Between the Strength of SiC-Mo Diffusion Couples and the Mechanical Properties of the Interfacial Reaction Products," Journal of Materials Science Letters, Vol. 15, 1996, pp. 307-310.

24. Schuster, J. C., "Silicon Nitride-Metal Joints: Phase Equilibria in the Systems Si_3N_4-Cr, Mo, W, and Re," Journal of Materials Science, Vol. 23, 1988, pp. 2792-2796.

25. Harmon, D. P., "Iridium-Base Alloys and Their Behavior in the Presence of Carbon," Technical Report No. AFML-TR-66-290, Oct. 1966.

26. Witcomb, M. J., Dahmen, U., and Westmacott, K. H., "A Study of Precipitation in Interstitial Alloys-II. A New Metastable Carbide Phase in Platinum," Acta Metallurgica, Vol. 31, No. 5, 1983, pp. 743-747.

27. Selman, G. L., Ellison, P. J., and Darling, A. S., "Carbon in Platinum and Palladium," Platinum Metals Review, Vol. 14, No. 1, January 1970, pp. 14-20.

28. Vines, R. F., "The Platinum Metals and Their Alloys," The International Nickel Company, Inc., New York, 1941.

29. Binary Alloy Phase Diagrams, ASM, 1986, vol.1, p. 583.

30. Binary Alloy Phase Diagrams, ASM, 1986, vol. 2, p. 1909.

31. Chou, T. C., "Anomalous Solid State Reaction Between SiC and Pt," Journal of Materials, Research, Vol. 5, No. 3, March 1990, pp. 601-608.

32. Chou, T. C., "High Temperature Reactions Between SiC and Platinum," Journal of Materials Science, Vol. 26, 1991, pp. 1412-1420.

33. Searcy, Alan W., and Finnie, Lies N., "Stability of Solid Phases in the Ternary Systems of Silicon and Carbon with Rhenium and the Six Platinum Metals," Journal of the American Ceramic Society, Vol. 45, No. 6, June 1962, pp. 268-273.

34. Criscione, J. M., Mercuri, R. A., Schram, E. P., Smith, A. W., and Volk, H. F., "High Temperature Protective Coatings for Graphite," Technical Document Report No. ML-TDR-64-173, Part II, Air Force Materials Laboratory, Wright-Patterson Air Force Base, Ohio, January 1965.

35. Isobe, Y., Yazawa, Y., Son, P., and Miyake, M., "Chemically Vapor-Deposited Mo/Re Double Layer Coating on Graphite at Elevated Temperatures," Journal of the Less-Common Metals, Vol. 152, 1989, pp. 239-250.

36. Arnoult, W. J., and McLellan, R. B., "The Solubility of Carbon in Rhodium, Ruthenium, Iridium, and Rhenium," Scripta METALLURGICA, Vol. 6, 1972, pp. 1013-1018.

37. Hamilton, J.C., Yang, N.Y.C., Clift, W.M., Boehme, D.R., McCarty, K.F., and Franklin, J.E., "Diffusion Mechanisms in Chemical Vapor-Deposited Rhenium," Metallurgical Transactions A, Vol. 23A, 1992, pp. 851-855.

38. Bose, A., and Schwab, S. T., "Analysis of Refractory Metal Samples," Southwest Research Institute, SwRI Project No. 06-4357, July 1991.

39. Govindarajan, S., Moore, J. J., Disam, J., and Suryanarayana, C., "Development of a Diffusion Barrier Layer for Silicon and Carbon in Molybdenum-a Physical Vapor Deposition Approach," Metallurgical and Materials Transactions A, Vol. 30A, 1999, pp. 779-806.

40. Govindarajan, S., Mishra, B., Olson, D. L., Moore, J. J., and Disam, J., "Synthesis of Molybdenum Disilicide on Molybdenum Substrates," Surface Coating Technology, Vol. 76-77, 1995, pp. 7-13.

41. Govindarajan, S., Moore, J. J., Aldrich, D. J., Ohno, T. R., Disam, J., Proc. 14th Int. Plansee Seminar, G. Kneringer, P. Rodhammer, and P. Wilharitz, eds., Plansee AG, Reutte, Tyrol, Austria, Vol. 1, 1997, pp. 720-730.

42. Hirvonen, J.-P., Kattelus, H., Suni, I., Likonem, J., Jervis, T. R. and Nastasi, M., "Mechanical Properties and Deformation Behavior of Materials Having Ultra-fine Microstructures," M. Nastasi, D. M. Parkin, and H. Gleiter,eds.,Kluwer Academic Publishers, Dordrecht, The Netherlands, 1993, pp. 469-474.

43. Mitchell, T. E., Nastasi, M., Jervis, T. R. and Kung, H., "Novel Techniques in Synthesis and Processing of Advanced Materials," J. Singh and S. M. Copley, eds., TMS. Warrendale, PA, 1995, pp. 271-281.

44. Kung, H., Jervis, T. R., Hirvonen, J.-P., Nastasi, M. and Mitchell, T. E., "High Temperature Silicides and Refractory Alloys," C. L. Briant, J. J. Petrovic, B. P. Bewlay, A. K. Vasudevan, and H. A. Lipsitt, eds., Mater. Res. Soc., Pittsburgh, PA, vol. 322, 1994, pp. 27-32.

45. Hirvonen, J.-P., Suni, I., Kattelus, H., Lappalainen, R., Torri, P., Kung, H., Jervis, T. R., and Nastasi, M., "High Temperature Silicides and Refractory Alloys," C. L. Briant, J. J. Petrovic, B. P. Bewlay, A. K. Vasudevan, and H. A. Lipsitt, eds., Mater. Res. Soc., Pittsburgh, PA, vol. 322, 1994, pp. 279-84.

46. Kung, H, Jervis, T. R., Hirvonen, J.-P., Embury, J. D., Mitchell, T. E., and Nastasi, M., "Structure And Mechanical-Properties Of $MoSi_2$-SiC Nanolayer Composites," Phil. Mag. A, 71A, 1995, pp. 759-779.

47. Dzyadykevich, Yu. V., "Scale-Resistant Coatings for Molybdenum and Molybdenum Base Alloys," Soviet Powder Metallurgy and Metal Ceramics, 27: (2), Feb. 1988, pp. 126-131.

48. Process Materials, 7083 Commerce Circle Suite E, Pleasanton, California 94588, website located at www.processmaterials.com/nitrides.html as of 04/01.

49. Sloof, W. G., Kooi, B. J., Delhez, R., de Keijser, Th. H., and Mittemeijer, E. J., "Diffraction Analysis of Nonuniform Stresses in Surface Layers: Application to Cracked TiN Coatings Chemically Vapor Deposited on Mo," Journal of Materials Research, Vol. No. 6, 1996, pp. 1440-1457.

50. Hwan, L., Kmetz, M., Suib, S. L. and Galasso, F. S., "Chemical Vapor Deposition of Tungsten and TiN on SiC Fibers," Journal of Materials Science, Vol. 27, 1992, pp. 2873-2876.

51. Ultramet, 12173 Montague Street, Pacoima, California 91331, website located at www.ultramet.com, as of 04/01.

52. Reed, B. D., Biaglow, J. A., Schneider, S. J., "Iridium-Coated Rhenium Radiation Cooled Rockets," NASA Technical Memorandum 107453, July 1997.

53. Reed, B. D., and Dickerson, R., "Testing of Electroformed Deposited Iridium/Powder Metallurgy Rhenium Rockets," NASA Technical Memorandum 107172, June 1996,

54. Reed, B. D., and Schneider, S. J., "Testing of Wrought Iridium/Chemical Vapor Deposition Rhenium Rocket," NASA Technical Memorandum 107452, July 1997.

Appendix: Literature Survey

The issues regarding material compatibility between ceramics and refractory metals have been a major focus of research over the past several years. In this regard, the need for diffusion barrier coatings for preventing the formation of deleterious carbides and silicides has been well documented. Advanced high-temperature cooling applications such as heat-pipe-cooled leading edges may often require the elevated-temperature capability of carbon/silicon carbide (C/SiC) or carbon/carbon (C/C) composites in combination with the hermetic capability of metallic tubes. In view of this, a critical review of past research efforts in the area of refractory metals incompatibility appears to be germane to identifying 1) potentially useful metal systems and 2) diffusion barrier coatings. Mo-Re alloys particularly are deemed potentially viable materials as heat-pipe-cooled leading edges in hypersonic vehicles. Compatibility of Mo-Re with silicon carbide and carbon is therefore a specific area of interest. By discussing previous research efforts on material incompatibilities, it is hoped that a clearer understanding would emerge as to which class of materials and coatings holds promise.

Refractory Metal Compatibility with Carbon and Silicon Carbide

Most refractory metals form carbides when in the presence of carbon at high temperatures. Nb, Ta, and Mo readily absorb C.[2-3] Carburization is expected for Mo above 2012°F, for W above 2552°F, and for Ta above 1832°F. The solid solubility of C in Mo varies between 0.005 and 0.0922 wt. % in the temperature range of 3002-3992°F,[4] with an activation energy, Q, for C in Mo being 163 Btu/mole in the temperature range of 2192-2912°F.[5] Re is the only refractory metal that does not form a carbide.[6-7] However, solubility of carbon in solid Re increases with temperature, resulting in excellent bond strength between carbon and Re. Re absorbs about 0.9 wt. % C when heated in methane at 1472-3992°F.

Lundberg[8] studied the interaction of SiC with W in the temperature range of 2916-3276°F. An electron microprobe analysis revealed the formation of W_5Si_3 and W_2C layers between the SiC deposition and the W substrate, i.e., a layered structure was formed comprised of SiC-W_5Si_3-W_2C-W. The two reaction layers appeared to grow at the same rate with no W diffusing into the SiC. Similarly, in graphite that was CVD coated with W and SiC a W_2C reaction layer was found between the W and the graphite, with no W in the graphite. From these studies, it was determined that SiC and C react with W at similar rates. The reaction layer growth could be predicted by

$$x = \sqrt{4.03 \times 10^4 \, (t) \, \exp(-113{,}400/T)}$$

where x is the reaction layer thickness in inches, t is the heating time in seconds, and T is the absolute temperature in degrees Rankine. As evident from the equation, reaction layer growth is highly temperature dependent.

Ranken and Lundberg[9-10] studied several different refractory metals for use in refractory-metal-lined ceramic tubes for heat pipes. The ceramics they chose for study were SiC and Al_2O_3. They looked for a refractory metal with a similar CTE as that of the ceramics. They determined that Nb and Al_2O_3 have nearly identical CTE's. In addition, W and either α- SiC or SiC containing 5-10 % free silicon (KT-SiC), have close CTE's. The CTE of β- SiC (the form typically obtained by CVD) can be fairly well matched by alloys of W and Mo. Similarly, CTE compatibility between CVD Niobium and Al_2O_3 was demonstrated by the absence of defects related to debonding and thermal stresses. Due to the uncertainty about the reaction between W and SiC, tests were performed on SiC with a CVD layer of W. Upon heating to 2916°F, three phases were revealed in

the reaction layer, W_5Si_3, W_6Si_2C, and W_6SiC_2. Si could not be detected in the W nor W in the SiC.

Merrigan and Keddy[11] studied SiC tubes with a CVD W liner for use in heat pipes for waste removal. SiC was used because it has excellent thermal shock resistance, good thermal conductivity, low volatility, and resistance to both oxidizing and reducing atmospheres. In addition, SiC has an extremely low hydrogen permeability and its CTE is similar to that of W. Previous investigations have shown the W-SiC reaction layer growth followed a parabolic law of the form $x^2 = 2Kt$, where x is the layer thickness, K is the reaction rate constant, and t is time.

Rovang, et al.,[12-13] reported on the development of a C/C heat-pipe internally coated with a Nb liner for the SP-100 project. Their approach was to use an interlayer of 0.039-0.197 mil (1-5 μm) thick Re (applied by CVD) between the C/C and the Nb. This interlayer would: a) provide a modest gradation of the CTE mismatch, b) assume a portion of the load from the induced stress, c) improve the coating adhesion, and d) serve as a carbon diffusion barrier to allow the Nb to remain ductile.

Yaney and Joshi[14] studied the reaction between Nb and SiC. A Nb layer, 0.0394-0.0787 mil (1-2 μm) thick, was sputter deposited on SiC substrates and heated to temperatures ranging from 1472 to 2323°F. An Auger electron spectroscopy depth profile revealed extensive reaction between the Nb and the SiC with the typical reaction layer sequence being $SiC/Nb_5Si_4C/Nb_5Si_3/Nb_2C/NbO/Nb$. Joshi, et al.,[15] studied the reaction of Nb and Ta with SiC and Al_2O_3 up to 2192°F. Nb and Ta were sputter deposited on SiC and Al_2O_3 substrates to a thickness of approximately 0.0394 mil (1 μm). The main thrust of their study related to the Nb/SiC system. They observed that the reactions of Nb with SiC was much more uniform for the single crystal SiC than for the polycrystalline SiC. Also, annealing the Nb/SiC system at 2012°F for 4 hr resulted in reaction of the entire Nb film. In contrast, there was no evidence of reaction in the Nb/Al_2O_3 system after heating at 2192°F for 4 hr, indicting that Al_2O_3 may be a good diffusion barrier between Nb and SiC.

Fries, et al.,[16] evaluated the diffusion of carbon into W and Mo. They found the diffusion of carbon through the carbide phase as the rate-determining step. Though a thin WC skin was observed, only the W_2C layer growth was prominent below 4352°F. The diffusion of W into carbon was negligible compared to that of C into W. Similarly, carbon diffusion into Mo was found to proceed rapidly, and the metal quickly became saturated with carbon.[16]

Reagan, et al.,[17-18] constructed tubes with a trilayer structure of SiC, graphite, and W. While the inside of the graphite tube was coated with W through CVD deposition, the outside of the tube was coated with CVD-deposited SiC. The mechanical integrity of the resulting structure was assessed by performing thermal shock, thermal cycling, and pressure tests. In one series of tests, one end of the structure was heated by radio frequency induction heating to 3853°F in air and then water quenched to below 1963°F. This process was repeated 10 times, with the structure remaining leak-tight. In another series of tests, the structure was cycled from 981°F to 2916°F in air by rf induction heating 150 times. Again, the structure remained leak tight. Next, the structure was cycled from 1000°F to 3177°F in air 102 times. A vacuum of 10^{-6} Torr was maintained inside the structure. During the last few cycles, a crack was noticed in the SiC, and testing was stopped to prevent oxidation of the W. The structure was also pressurized to 500 psi for several hours and remained leak tight.

The feasibility of coating C/C tubes internally with refractory metals for use as heat pipes was studied by Hartenstine et al.[19] Re was used as a carbon diffusion barrier coating between the C/C and the refractory liner (either W or Nb). Four different coating techniques were studied. A 0.002

in. thick layer of carbon was applied between the C/C and the Re to transition the CTE between them and thereby reduce the interfacial thermal stresses. Though Re does not form a stable carbide at their use temperature of 2804°F, carbon was found to diffuse through the Re and react with the W or the Nb substrates, to form a W-carbide or a Nb-carbide. As the coatings were applied at a temperature of 1832°F or higher, the most severe thermal stresses were experienced during the cooling of the systems. Re/W and the C/Re/W coatings cracked severely during thermal cycling due to the embrittlement of the W as a result of carbon diffusion through the Re. The Re/W coating separated from the C/C wall, while the C/Re/W coating did not. The Re/Nb and C/Re/Nb coatings completely separated from the wall to form an almost stand-alone tube with only minor cracking. Again, the carbon diffused through the Re, this time resulting in Nb-carbides.

Rabin[20] reviewed the interaction of SiC with various metals (Ni, Fe, Ti, Cr, Al, Cu, Pd, Mo, W, V, Ta, Nb, Hf and Zr) with relevance to SiC joining. In the SiC/Mo system, Mo_2C formed as a result of C diffusion into the Mo, together with a small amount of Mo_5Si_3 in between the SiC and the carbide layer. In yet another study, a Mo_2C layer, a mixed layer of Mo_2C + Mo_5Si_3, and a layer of Mo_5Si_3C were found to grow between the Mo and SiC. In the SiC/W system, existence of a mixed layer of W-carbide + W-silicide was noticed.

In graphite coated with Mo, growth of an Mo_2C intermediate layer was observed between the graphite and Mo[21]. This carbide layer had a parabolic growth rate with annealing time, at temperatures as high as 1832°F. Cross-sections of the Mo coating revealed the Mo grains to be columnar in structure, with grain size increasing with deposition temperature. The diffusion coefficient of C in Mo was found to increase with decreasing columnar grain size; and experimentally determined diffusion coefficients as well as carbide growth rates for a Mo coating on graphite, and for a Mo sheet coupled to graphite, were documented. The study concluded that for Mo coatings on graphite, grain boundary diffusion of C in the carbide layer played a significant role in the carbide layer growth.

Diffusion couples of Mo and Si were used by Tortorici and Dayananda[22] to study the growth of silicides and interdiffusion in a Mo-Si system. The diffusion couples were heat-treated in either a H_2 atmosphere at temperatures between 1652°F and 2012°F, or in an Ar-5% H_2 atmosphere at temperatures up to 2462°F. Layers of $MoSi_2$ and Mo_5Si_3 were observed in each case. The $MoSi_2$ grains exhibited a preferred direction of growth parallel to the diffusion direction. Also, the $MoSi_2$ layer exhibited a columnar microstructure and had one to two orders of magnitude greater thickness than the Mo_5Si_3 layer. The interdiffusion coefficients of Mo and Si were also one to two orders of magnitude greater than in both $MoSi_2$ and Mo_5Si_3. No Mo_3Si was found, however, despite the fact the Mo-Si phase diagram allows its formation. Since Mo_3Si was observed by other researchers to have formed at temperatures above 2552°F, Tortorici and Dayananda suggest that barriers for the nucleation of Mo_3Si are perhaps overcome at higher temperatures.

Martinelli et al.[23], studied diffusion couples of Mo and SiC. The Mo-SiC joints were made by hot pressing at temperatures between 2192ºF and 2732ºF for times between 15 minutes and 2 hours. The reaction layer that formed consisted of a mixed layer of Mo_5Si_3 and Mo_2C. Hot-pressing for longer times at lower temperatures (i.e., 2 hr at 2372ºF) resulted in a separate and distinct layer of Mo_2C being extended into the Mo region. On the other hand, on hot pressing at 2552ºF for long times or at 2732ºF, a layer of Mo_5Si_3C formed against the SiC interface. Shear strengths of the joints as a function of hot pressing times of 15 min, 30 min, 1 hr, and 2 hr were determined. At 2192ºF, shear strength increased as bonding times increased. At 2372ºF, shear strength increased for times up to 1 hr and decreased thereafter for the 2 hr exposure. While at 2552ºF, no specific trend was apparent, at 2732ºF, shear strengths showed a continuous decline with increasing hot pressing times. The authors attributed these trends in shear strength to the variations of elastic moduli and the CTE of the Mo, SiC, and inter-layers. The Mo_2C layer was said to be compatible with SiC. Therefore strength increased with time at low temperatures where Mo_2C

formed. In contrast, the SiC and Mo_5Si_3 layers, as well as the SiC and Mo_5Si_3C layers were deemed mutually incompatible, and hence strength decreased for the higher temperature exposures where these incompatible silicides formed[23].

The phase equilibria of Si_3N_4 with Cr, Mo, W, and Re were studied by Schuster[24], at temperatures of 1832°F and 2552°F in an argon environment. In addition, he complemented his study with a critical review of the available literature. In the Cr-Si-N system, Si_3N_4 reacted with chromium at temperatures as low as 1652°F. Various chromium silicides, such as $CrSi_2$, CrSi, Cr_5Si_3, and Cr_3S formed. In the absence of external nitrogen pressure, Cr_2N did not form. However, it did form when there was a sufficient nitrogen partial pressure resulting from the decomposition of Si_3N_4 by chromium. In the Mo-Si-N system, in the absence of a nitrogen pressure, $MoSi_2$ and Mo_5Si_3 formed and co-existed with Si_3N_4 at 1832°F. Reactions between Si_3N_4 and Mo were slow. At temperature of 2912°F and higher, however the co-existence between Si_3N_4 and Mo_5Si_3 was disturbed and only $MoSi_2$ co-existed with nitrogen gas. In the W-Si-N system under an argon environment, reactions between tungsten and Si_3N_4 did not occur at the temperature of 1832°F. At a higher temperature of 2143°F, however, reactions caused the formation of nitrogen and W_5Si_3; and at a still higher temperature of 2732°F, nitrogen also co-existed with WSi_2. In the Re-Si-N system, Si_3N_4 did not react with Re in argon at the temperature of 1832ºF. However, at 2552°F, $Re_{17}Si_9$ and nitrogen gas formed. In assessing the viability of Si_3N_4 as a diffusion barrier coating in these metallic systems, Schuster concluded that the formation of the various embrittling silicides, together with the undesirable chemical reactions occurring during thermal cycling, restrict the potential of such joints for structural applications at elevated temperatures.

Carbon Diffusion Barriers

Potential diffusion barrier coatings for refractory metals in contact with carbon, appear to be Pt, Ir, Re, SiC, TiB_2 and TiC. Platinum forms low melting silicides at rather low temperatures, and this restricts its use in a C/SiC composite.[25] Carbon forms a eutectic with Pt at 3150°F; with Ir at 4177°F (but this temperature is significantly lowered in the presence of Si to at least 3902°F); and with Re at 4471°F. It is thought that while Re does not form a carbide, carbon has been found to diffuse through a Re coating and cause embrittlement of the substrate metal.[19] However, the diffusion of carbon through Re is temperature dependent, and is not thought to be significant up to 3000°F. The TiB_2 coating, on the other hand, appears to prevent diffusion of carbon through it, but its efficacy has not been tested at high temperatures and for extended time periods. TiC coating is thought to be an effective diffusion barrier for carbon, but its utility is limited by its severe brittleness.

Platinum, Iridium, and Rhenium

Interactions of Pt and Ir with carbon were studied by Whitcomb, et al.[26] and Selman et al[27]. Molten Pt (and others in its group) dissolves substantial amounts of carbon, which in turn depresses the melting point of Pt. Pt and C form a eutectic at a temperature slightly below the melting point of Pt. The eutectic solidification is characterized by the formation of a mixture containing a near C-free Pt solid solution and graphite. Pt containing the eutectic graphite is brittle.[28] In contrast to most reports that the solubility of C in Pt is small[26] (~1 wt.% max. at 1700°C)[29], Pt dissolves substantial amounts of C after heating in contact with graphite powder for a few hours even at temperatures as low as 2192°F.[27] While the dissolved C in solid Pt has little effect on the hardness of Pt, the dissolved C in Pd considerably increases the hardness of Pd. It is also reported that at high temperatures, carbon diffuses very rapidly in solid Pt.[27]

Pt and Si form three eutectics over the entire compositional range with melting temperatures ranging from 1497-1810 °F.[30] Pt that contains sufficient Si to form the low melting eutectic phase is brittle.

Chou[31] studied the reaction between Pt and SiC at 1652°F and reported interfacial melting between Pt and SiC due to a reaction product with a low melting point. The further annealing at 1652°F caused the reaction zone to penetrate into the SiC. All the SiC decomposed in that region converted into a mixture of Pt_3Si (with a melting point of 1526°F) and C. In another study, extensive reaction between SiC and Pt were observed to take place in the temperature range of 1652-2012°F.[32] The reaction products were graphite and Pt-silicides. Local melting followed by solidification was observed at the interface, with formation of Pt-silicides. Due to its low solubility in Pt-silicides, the carbon precipitated out of the Pt-silicide matrix.

Searcy and Finnie[33] studied the ternary systems of Si and C with Re and the Pt metals. They observed that neither the Pt metals nor Re formed stable compounds with C at temperatures up to 2912°F. Rhenium silicides were observed to be less stable than silicides of the Pt metals.

The CTE of Ir closely matches with that of Mo, W, and Ta, and can therefore be recommended as a good oxidation diffusion barrier.[34] Ir does not form a carbide at temperatures up to 3812°F. The diffusion rate of carbon in Ir at temperatures up to 3452°F is low; but above this temperature, the diffusion rate is high.

A strong bond can be formed between Ir and C by allowing molten Ir to wet the surface of a graphite substrate.[34] The bonding results from a dissolution of graphite in the molten Ir (at ~3992°F) with subsequent reprecipitation of the graphite upon solidification of the metal. The graphite crystallites form an interlocking network with the Ir and the graphite substrate.

Interactions of Ir-base alloys with carbon were studied by Harmon.[25] There is an Ir-C eutectic at 4177°F (melting point of Ir is 4429°F), and this temperature is significantly lowered in the presence of silicon to at least 3902°F.

The effectiveness of a Re coating as a diffusion barrier between a graphite substrate and a Mo coating was investigated. The Re coatings were 1.5-20 μm while the Mo coatings were 10 μm thick. Graphite samples coated with Mo, and with both Re and Mo, were annealed at temperatures from 1652°F - 2192°F. It was found that the growth of the Mo_2C interlayer depended greatly on the thickness of the Re layer, with the reaction rate decreasing exponentially with increasing Re layer thickness. In both the single layer coating of Mo and the double layer coating of Re/Mo, the growth of the intermediate carbide layer obeyed a parabolic law with annealing temperature. At lower temperatures, the Re layer was more effective in slowing down the growth rate of the carbide layer. For the case of a 10 μm Re interlayer, the carbide layers were 4, 23, 56, and 69% as thick as for the a single Mo layer, at annealing temperatures of 1652, 1832, 2012, and 2192°F respectively. Grain size or thickness of its columnar structure also had an effect on the reaction rate of carbide growth. The carbide layer increased in thickness with decreasing grain size of the Re layer. It is believed that columnar grain boundaries in the Re layer act as fast diffusion paths for carbide layer growth in the Mo layer[35].

Arnoult and McLellan[36] studied the solid solubility of carbon in several refractory metals such as Rh, Ru, Ir, and Re. Metal foil samples in contact with graphite were annealed at temperatures in the range of 1508°F-2293°F, until equilibrium had been reached. Carbon content was determined by a combustion C-analysis method using NBS (National Bureau of Standards) standards for calibration. The solubility of carbon in the four metals was low and increased with temperature. Solubility is defined as the atom ratio of carbon to metal. Carbon was the least soluble in Ir, followed by that in Rh, Ru, and Re, with carbon solubilities in Ir being several times

lower than for the other metals, with the difference being predominant at high temperatures. In rhenium, the solubility of carbon ranged from 8.52E-4 at 1508ºF to 170.0E-4 at 2293ºF. The solubility of carbon in rhodium ranged from 8.70 x 10^{-4} at 1508ºF to 75.0 x 10^{-4} at 2293ºF with a peak of 118.0 x 10^{-4} occurring at the intermediate temperature of 2156ºF. In the carbon-iridium system, the solubility of carbon ranged from 3.28 x 10^{-4} at 1508ºF to 25.2 x 10^{-4} at 2293ºF. The solubility of carbon in ruthenium ranged from 9.95 x 10^{-4} at 1508ºF to 125.0 x 10^{-4} at 2293ºF.

Hamilton et al[37]. characterized diffusion-related changes in samples taken from a Mo thruster manufactured by CVD. The thruster consisted of a Mo mandrel and had a 50 μm Ir coating followed by a 2 mm Re coating on it. The Mo mandrel was etched away after the thruster was fabricated. In an un-annealed sample taken from the thruster, a 3 μm Ir-Re interdiffusion layer, and two interdiffusion layers of IrMo and Ir_3Mo (2-3 μm in total thickness) were observed. In addition, adjacent to the Ir/Re interface, a 40 μm region of the Re coating, containing small voids was also evident. X-ray diffraction analysis of the un-annealed sample showed the average grain size in the Ir coating to be 10 μm while that in the Re layer to be ~400 μm. From three annealed samples (2552°F for 14 hours, 3092°F for 8 hours, and 3452°F for 8 hours), it was determined that no significant grain growth occurred during extended anneals at temperatures up to 2452°F. However, additional void growth was observed for the sample annealed at 2452ºF. The width of the interdiffusion zone in which Re diffused into Ir increased with temperature and had widths of 10 μm, 20 μm, and 40 μm at temperatures of 2552°F, 3092°F, and 3452°F respectively.

Titanium Diboride

TiB_2 coatings on Mo-Re, to serve as diffusion barriers for use between Mo-Re and C, were developed by the Advanced Technology Coatings, Ft. Worth, TX. Results of the study on interdiffusion of carbon were reported for Mo-Re coated with carbon, Mo-Re coated with TiB_2/C, and Mo-Re coated with TiB_2/C/SiC.[38] These alloy samples had not been heated except during the CVD process. Results of this study are summarized as follows. In the Mo-Re sample coated only with C, Mo diffused into the C coating, but no C diffused into the substrate. In addition, no cracks were detectible at the coating-substrate interface. In the Mo-Re sample coated with TiB_2/C, no C was detected in the substrate; also, no cracks were visible at the coating-substrate interface. Next to the substrate, a Ti-rich layer was seen. Neither C or Mo was observed in the TiB_2 layer. Diffusion of Mo from the substrate into the C was not apparent. Detection of B in the inter-layers and also the substrate was extremely difficult. In the Mo-Re sample coated with TiB_2/C/SiC, the outer surface showed only Ti. It was believed that the C and SiC layers had broken off during metallographic sample preparation. No C or Ti was detected in the substrate, however.

Molybdenum Disilicide

Govindarajan et al[39], investigated coating systems that had the potential to provide oxidation protection and prevent the C and Si diffusion into a Mo substrate. They pointed out the problems associated with using $MoSi_2$ as a diffusion barrier. The CTE of $MoSi_2$ does not match that of a Mo substrate (CTE at 1832ºF for $MoSi_2$ is reported to be 5.2 x 10^{-6} F^{-1} while for Mo it is 3.7 x 10^{-6} F^{-1}). In addition, $MoSi_2$ exhibits low creep strength at high temperatures, with the diffusion of Si into Mo promoting the embrittling silicides.[39] A multilayer coating of Mo and Si was used to alleviate the CTE mismatch. The reasoning was that silicon, in excess of that necessary for forming stoichiometric $MoSi_2$, would minimize the formation of silicides. However excessive silicides did form.[40] Efforts at matching the CTE of Mo by using a layer of $MoSi_2$ + 1.96 moles SiC was not beneficial, either. Annealing at 1832ºF caused the formation of Mo_3Si and Mo_5Si_3 with a resulting deleterious change in the CTE of the silicides layer.[41] Based on this work, a new coating system

was developed. The new coating system consisted of a Mo substrate that was coated with a diffusion barrier (based on the Mo-Si-C-N quaternary system) to prevent the diffusion of C and Si into the substrate. On top of the diffusion barrier layer, a layer of $MoSi_2$ + 1.96 moles SiC was applied. This was followed by a thick layer of B- and Ge-doped $MoSi_2$. The doping helps to lower the viscosity of the glassy, self-healing oxide (SiO_2) that forms on the surface as the $MoSi_2$ layer oxidizes. This silica scale serves as a diffusion barrier for oxygen. The diffusion barrier applied onto the Mo substrate was chosen based on promising results by a research group at Los Alamos National Laboratory and the Technical Research Center of Finland in which $MoSi_2N_x$ prevented the formation of silicides up to 1652ºF (the highest temperature investigated).[42-46] The diffusion barrier used by Govindarajan et al.[39], was reactive sputtered onto the Mo substrate. It was comprised of Mo-Si-C-N, and had an undetermined stoichiometry of $MoSi_xN_yC_z$. Annealing was conducted in a vacuum at 1832ºF (the highest temperature investigated) for 30 minutes. Silicides and carbides did not form in the Mo substrate. The effectiveness of the diffusion barrier layer in preventing the diffusion of C and Si was attributed to its amorphous nature. A powder form of the Mo-Si-C-N diffusion barrier as well as a sample of Mo foil coated with the Mo-Si-C-N diffusion barrier layer and the $MoSi_2$ + 1.96 moles SiC composite layer were stable up to temperatures of 2300ºF in an oxidizing environment. The authors[39] suggest that a promising area of investigation would be the amorphous layers of nitrided refractory metal silicides in the form of $M_5Si_3N_x$, where M represents Ta, W, Mo, etc. It was recommended that Ta_5Si_3 would be a good silicide to nitride since it is one of the best Si diffusion barriers among these silicides, which are more effective Si diffusion barriers than the MSi_2 silicides.[47]

Overview

Incompatibility between Mo-Re and other refractory materials, in the form of joints and coatings, can degrade the mechanical properties of Mo-Re. Two major issues of incompatibility include chemical incompatibility and the CTE mismatch. While chemical incompatibility can lead to embrittlement of Mo-Re through formation of carbides and/or silicides, the CTE mismatch can lead to a poorly protected or an exposed Mo-Re substrate with inadequate protection against a hostile oxidizing service environment.

The literature review conducted hitherto has facilitated identification of compatibility issues, classes of materials that poorly match with Mo-Re, and those materials that hold promise as diffusion barriers. As a general rule, all sources of C and Si that lead to formation of detrimental carbides and silicides in Mo-Re should be avoided. However, a silicon-bearing system such as the $M_5Si_3N_x$ may still be worth considering as a diffusion barrier.[47] Ceramic coatings of nitrides or borides are also an area worth exploring. Nitrogen has been observed to be compatible with several refractory metals.[23] Potentially useful nitrides are ZrN, TiN, HfN, and BN. These nitrides have fairly high melting points (2980°C, 2930°C, 2852°C, and 2300ºC respectively), and have relatively low densities compared to nitrides such as the TaN.[48] Some work has been done with TiN coatings on Mo and SiC. It appears that the relatively high CTE of TiN may preclude its use, unless an appropriate intermediate layer that provides a transition in thermal expansions is used.[49-50] Possible useful borides are HfB_2, TaB_2, W_2B_2, ZrB_2, and TiB_2. A critical literature review of these borides, with particular reference to their chemical and thermal expansion compatibilities, may help narrow the scope of future developmental studies.

Issues of concern in targeting elements from the Pt group as possible diffusion barrier coatings are density, CTE, temperature capability, and material compatibility. Even though a certain metal does not react with C and/or Si, it may not necessarily render itself as a suitable candidate material for diffusion barrier coating. For example, Re is not very reactive with C or Si, but C and Si can easily diffuse through the Re layer into the Mo substrate, and form substrate Mo carbides and/or silicides.

From the Pt group of metals, Os, Ir, and Ru (with respective density, CTE, and melting points of 22.2 g/cm^3, 2.8 ppm/ºF and 5513ºF for Os; 22.4 g/cm^3, 3.6 ppm/ºF and 4370ºF for Ir; and 12.2 g/cm^3, 3.6 ppm/ºF and 4190ºF for Ru[51]), are potential candidates as diffusion barrier coatings between Mo-Re, carbon, and SiC. Ir is a viable diffusion barrier coating due to its proven track record as a rocket thruster coating material, and also due to its favorable compatibility with Re[52-54]. Pt and Pd, on the other hand, may not serve as useful candidate diffusion barrier coatings materials. This is because they have relatively low melting points and relatively high CTE (with respective density, CTE, and melting point of 21.4 g/cm^3, 4.9 ppm/ºF and 3222ºF for Pt; and 12.0 g/cm^3, 6.5 ppm/ºF and 2826ºF for Pd[51]). Also, carbides that form through interaction of Pt and C have even lower melting points than Pt.

REPORT DOCUMENTATION PAGE

Form Approved
OMB No. 0704-0188

1. AGENCY USE ONLY *(Leave blank)*	2. REPORT DATE	3. REPORT TYPE AND DATES COVERED
	December 2001	Technical Memorandum

4. TITLE AND SUBTITLE
Effectiveness of Diffusion Barrier Coatings for Mo-Re Embedded in C/SiC and C/C

5. FUNDING NUMBERS
WU 242-33-03-20

6. AUTHOR(S)
David E. Glass, Ravi N. Shenoy, Zengmei Wang, and Michael C. Halbig

7. PERFORMING ORGANIZATION NAME(S) AND ADDRESS(ES)
NASA Langley Research Center
Hampton, VA 23681

8. PERFORMING ORGANIZATION REPORT NUMBER
L-18116

9. SPONSORING/MONITORING AGENCY NAME(S) AND ADDRESS(ES)
National Aeronautics and Space Administration
Langley Research Center
Hampton, VA 23681-2199

10. SPONSORING/MONITORING AGENCY REPORT NUMBER
NASA/TM-2001-211264

11. SUPPLEMENTARY NOTES
Glass: Langley Research Center, Hampton, VA; Shenoy, Lockheed Martin Engineering & Sciences, Hampton, VA; Wang, Chromealloy Gas Turbine Corporation, Orangeburg, NY; Halbig, Glenn Research Center, Cleveland, OH.

12a. DISTRIBUTION/AVAILABILITY STATEMENT
Unclassified-Unlimited
Subject Category 24 Distribution: Nonstandard
Availability: NASA CASI (301) 621-0390

12b. DISTRIBUTION CODE

13. ABSTRACT *(Maximum 200 words)*
Advanced high-temperature cooling applications may often require the elevated-temperature capability of carbon/silicon carbide or carbon/carbon composites in combination with the hermetic capability of metallic tubes. In this paper, the effects of C/SiC and C/C on tubes fabricated from several different refractory metals were evaluated. Though Mo, Nb, and Re were evaluated in the present study, the primary effort was directed toward two alloys of Mo-Re, namely, arc cast Mo-41Re and powder metallurgy Mo-47.5Re. Samples of these refractory metals were subjected to either the PyC/SiC deposition or embedding in C/C. MoSi2(Ge), R512E, and TiB2 coatings were included on several of the samples as potential diffusion barriers. The effects of the processing and thermal exposure on the samples were evaluated by conducting burst tests, microhardness surveys, and scanning electron microscopic examination (using either secondary electron or back scattered electron imaging and energy dispersive spectroscopy). The results showed that a layer of brittle Mo-carbide formed on the substrates of both the uncoated Mo-41Re and the uncoated Mo-47.5Re, subsequent to the C/C or the PyC/SiC processing. Both the R512E and the MoSi2(Ge) coatings were effective in preventing not only the diffusion of C into the Mo-Re substrate, but also the formation of the Mo-carbides. However, none of the coatings were effective at preventing both C and Si diffusion without some degradation of the substrate.

14. SUBJECT TERMS
Coatings; Composites; Carbon diffusion barrier; Silicon

15. NUMBER OF PAGES
46

16. PRICE CODE

17. SECURITY CLASSIFICATION OF REPORT	18. SECURITY CLASSIFICATION OF THIS PAGE	19. SECURITY CLASSIFICATION OF ABSTRACT	20. LIMITATION OF ABSTRACT
Unclassified	Unclassified	Unclassified	